Research Paper

GEOSPHERE

GEOSPHERE; v. 12, no. 3

doi:10.1130/GES01252.1

12 figures; 2 tables; 2 supplemental tables

CORRESPONDENCE: gwenlinde@yahoo.com

CITATION: Linde, G.M., Trexler, J.H., Jr., Cashman, P.H., Gehrels, G., and Dickinson, W.R., 2016, Detrital zircon U-Pb geochronology and Hf isotope geochemistry of the Roberts Mountains allochthon: New insights into the early Paleozoic tectonics of western North America: Geosphere, v. 12, no. 3, p. 1016–1031, doi:10.1130/GES01252.1.

Received 17 August 2015
Revision received 21 November 2015
Accepted 26 February 2016
Published online 7 April 2016

THE GEOLOGICAL SOCIETY OF AMERICA®

Detrital zircon U-Pb geochronology and Hf isotope geochemistry of the Roberts Mountains allochthon: New insights into the early Paleozoic tectonics of western North America

Gwen M. Linde[1], **James H. Trexler, Jr.**[1], **Patricia H. Cashman**[1], **George Gehrels**[2], **and William R. Dickinson**[2,*]

[1]Department of Geological Sciences and Engineering, University of Nevada, Reno, Nevada 89557-0172, USA
[2]Department of Geosciences, University of Arizona, Tucson, Arizona 85721-0077, USA

ABSTRACT

Detrital zircon U-Pb geochronology and Hf isotope geochemistry provide new insights into the provenance, sedimentary transport, and tectonic evolution of the Roberts Mountains allochthon strata of north-central Nevada. Using laser-ablation inductively coupled plasma mass spectrometry, a total of 1151 zircon grains from six Ordovician to Devonian arenite samples were analyzed for U-Pb ages; of these, 228 grains were further analyzed for Hf isotope ratios. Five of the units sampled have similar U-Pb age peaks and Hf isotope ratios, while the ages and ratios of the Ordovician lower Vinini Formation are significantly different. Comparison of our data with that of igneous basement rocks and other sedimentary units supports our interpretation that the lower Vinini Formation originated in the north-central Laurentian craton. The other five units sampled, as well as Ordovician passive margin sandstones of the western Laurentian margin, had a common source in the Peace River Arch region of western Canada. We propose that the Roberts Mountains allochthon strata were deposited near the Peace River Arch region, and subsequently tectonically transported south along the Laurentian margin, from where they were emplaced onto the craton during the Antler orogeny.

INTRODUCTION

The Roberts Mountains allochthon (RMA) consists of internally deformed Cambrian through Devonian rocks, and structurally overlies coeval passive margin strata in northeastern and north-central Nevada (Schuchert, 1923; Kay, 1951; Roberts et al., 1958; Madrid, 1987; Burchfiel et al., 1992) (Figs. 1 and 2). Roberts Mountains allochthon rocks include chert, argillite, arenite, quartzite, limestone, and mafic volcanic rocks. The RMA is often thought to have been deposited in an ocean basin outboard of coeval passive margin strata in western Laurentia and to have been tectonically emplaced onto this margin during the Late Devonian to Early Mississippian Antler orogeny (e.g., Roberts et al., 1958; Burchfiel and Davis, 1972; Madrid, 1987). Various workers have suggested wildly disparate sources for the RMA strata. Some workers (e.g., Roberts et al., 1958; Burchfiel and Davis, 1972; Poole et al., 1992) suggested that the RMA strata originated in western Laurentia (Fig. 1) and deposited in an ocean basin to the west. Speed and Sleep (1982) hypothesized that the RMA strata are the accretionary prism of a far-traveled arc. Gehrels et al. (2000a) proposed that the RMA originated in the Peace River Arch region of western Canada. Wright and Wyld (2006) suggested that the RMA was deposited as far afield as Avalonia or Gondwana and subsequently was tectonically transported to western Laurentia along its southern margin (Fig. 3). Colpron and Nelson (2009) proposed that RMA strata could have originated in the northern Baltica–southern Caledonides region and been tectonically transported along the northwest margin of Laurentia (Fig. 3). Determining the provenance of the RMA units will unravel this puzzle and provide new insight into early Paleozoic tectonics in the western Cordillera.

The gaps in understanding about the RMA strata—their provenance, sedimentary transport to depositional basin, and possible subsequent tectonic transport—can be addressed using detrital zircon analyses. We analyzed detrital zircons to obtain both uranium-lead ages and hafnium isotope ratios. U-Pb ages are important for identifying and then characterizing the provenance of sedimentary strata, and for comparison between sedimentary units (Gehrels et al., 2000b; Fedo et al., 2003; Gehrels, 2012, 2014). Hafnium isotope compositions are used to determine the geochemical character of the magma in which the zircons crystallized. When combined with U-Pb ages, Hf isotope composition provides a powerful complement for interpreting sedimentary provenance (Bahlburg et al., 2011; Gehrels and Pecha, 2014).

In this study, we determined the U-Pb ages and Hf isotope compositions of detrital zircons in six samples of RMA strata in north-central Nevada. We use these data to interpret provenance, sedimentary transport to depositional basins, possible subsequent tectonic transport, and relationships between RMA units. Our study builds on an earlier analysis of RMA samples that determined U-Pb ages using isotope-dilution–thermal ionization mass spectrometry (ID-TIMS) (Gehrels et al., 2000a, 2000b). Using detrital zircons from the same samples, the original data set was enlarged and enhanced.

---

*Deceased.

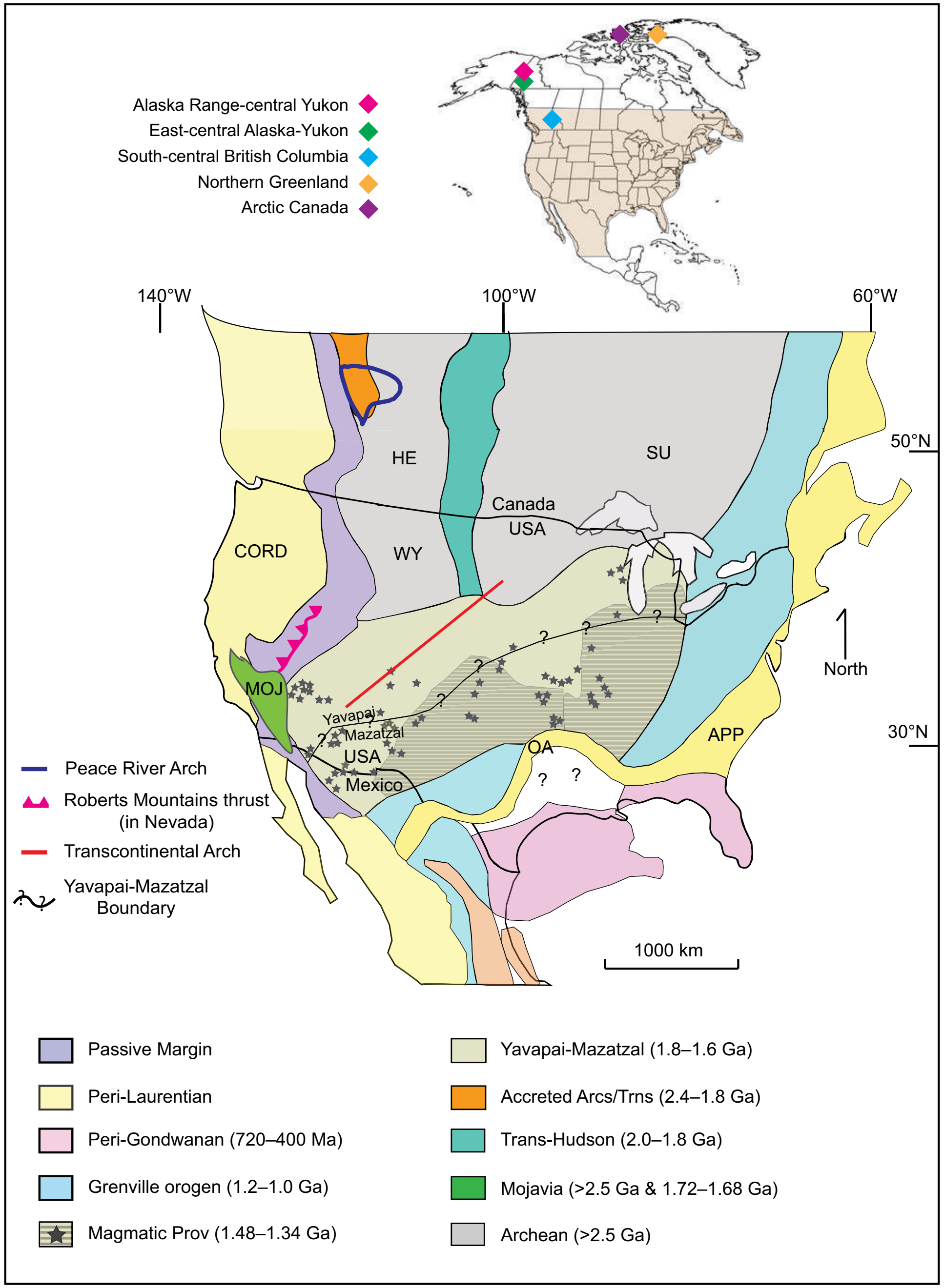

Figure 1. Locations of the main age provinces in North America that are potential source terranes for western Laurentian strata. The location of Transcontinental Arch is shown as a red line (Sloss, 1988); the Peace River Arch is shown as a blue line. The trace of the Roberts Mountains thrust is shown. WY—Wyoming province; HE—Hearn province; SU—Superior province; CORD—Cordilleran; APP—Appalachian; OA—Ouachita-Marathon; MOJ—Mojavia. Figure is after Gehrels et al. (2011) and compiled from Bickford et al. (1986), Hoffman (1989), Ross (1991), Burchfiel et al. (1992), Anderson and Morrison (1992), Bickford and Anderson (1993), Van Schmus et al. (1993), Villeneuve et al. (1993), Dickinson and Lawton (2001), Whitmeyer and Karlstrom (2007), and Dickinson and Gehrels (2009). An inset map of North America shows other locations referred to in the text.

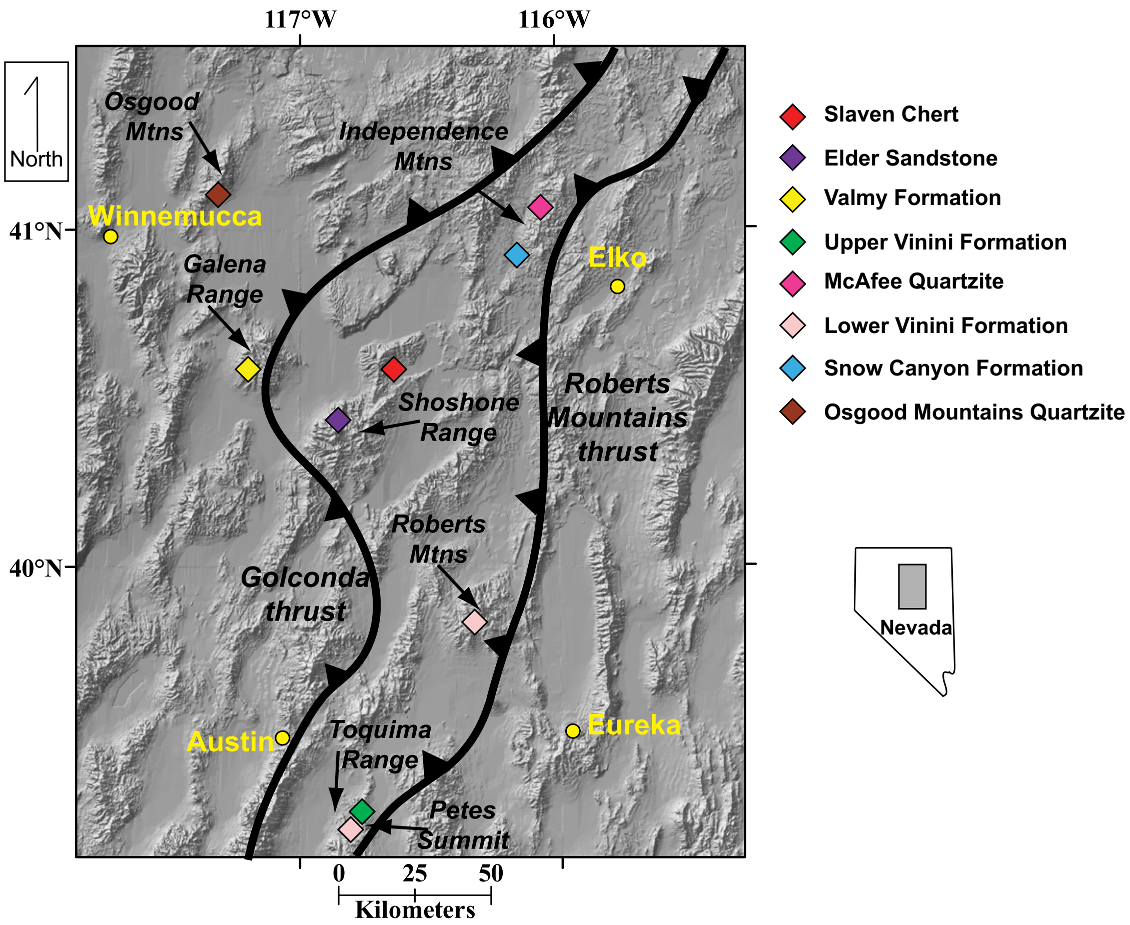

Figure 2. Map of north-central Nevada, showing sample locations (colored symbols) and the traces of the Roberts Mountains and Golconda thrusts. Some Roberts Mountains allochthon (RMA) rocks crop out to the west of the Golconda thrust in tectonic windows through the allochthon. Antler orogenic highlands are the map area to the west of the Roberts Mountains thrust; Antler Foreland Basin is the map area to the east of the Roberts Mountains thrust. Thrust traces are after Dickinson (2006); Antler highlands and basin are after Poole (1974).

We analyzed a significantly larger number of grains per sample, changed and updated grain selection methods, and added Hf isotope composition analyses. We used laser-ablation–inductively coupled plasma mass spectrometry (LA-ICPMS) for all analyses. We report here 1151 new U-Pb ages and 228 new Hf isotope analyses.

Detrital zircon analyses allow us to resolve the original sources of these units. We show that some RMA units in some cases share an origin, while others units do not.

GEOLOGIC SETTING

Regional Tectonostratigraphic Framework

The North American craton contains several Proterozoic and Archean age provinces, thus providing geologically distinguishable crustal provinces that are source terranes for the upper Proterozoic and lower Paleozoic continental margin sedimentary section (e.g., Gehrels et al., 2011, and references cited

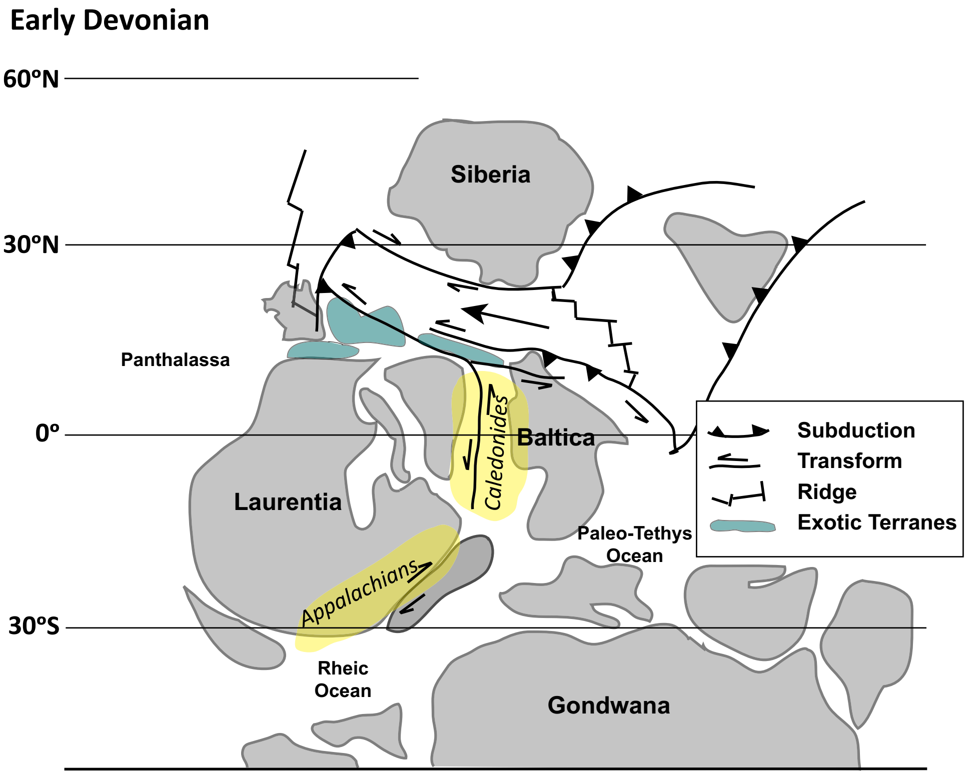

Figure 3. Early Devonian "Northwest Passage" between Laurentia, Baltica, and Siberia proposed by Colpron and Nelson (2009). Exotic terranes include the Alexander, Klamath, and northern Sierran terranes. Map is after Colpron and Nelson (2009).

therein) (Fig. 1). The Yavapai-Mazatzal Province (1.8–1.6 Ga) extends across central North America (Fig.1). It is bounded on the north and northwest by the Trans-Hudson orogenic terrane (2.0–1.8 Ga) and Archean rocks (>2.5 Ga) of the Wyoming and Superior Provinces (Fig. 1). It is bounded on the south and east by the terranes of the Grenville orogen (1.2–1.0 Ga) and on the west by the Mojavia terrane (>2.5 Ga with 1.6–1.7 Ga granitoids) (Fig. 1).

Detrital zircon sources for the passive margin section changed in the upper Proterozoic–Lower Cambrian (Linde et al., 2014, and references cited therein). The 1.2–1.0 Ga Grenville orogen of southern and eastern North America (Fig. 1) was a significant sediment source for western Laurentia throughout the Neoproterozoic (Rainbird et al., 1997, 2012), including the upper Proterozoic passive margin section from the northwest United States to Sonora, Mexico (e.g., Lawton et al., 2010; Gehrels and Pecha, 2014; Yonkee et al., 2014; Linde et al., 2014). In contrast, the 1.8–1.6 Ga Yavapai-Mazatzal and 1.48–1.34 Ga mid-continent granite-rhyolite provinces within the North America craton (Fig. 1) were the more predominant sediment sources for strata higher in the passive margin section (e.g., Lawton et al., 2010; Gehrels and Pecha, 2014; Yonkee et al., 2014; Linde et al., 2014).

The RMA is often interpreted as a package of oceanic sediments emplaced structurally eastward onto the western Laurentian craton during the Late Devonian–Early Mississippian Antler orogeny (Roberts et al., 1958; Poole et al., 1992). Roberts Mountains allochthon strata are exposed in north-central Nevada between the Golconda thrust on the west and the Roberts Mountains thrust on the east; some units crop out west of the Golconda thrust in tectonic windows (Fig. 2). Rocks of the allochthon structurally overlie coeval rocks of the western Laurentian passive margin (e.g., Schuchert, 1923; Kay, 1951; Roberts et al., 1958; Madrid, 1987) (Fig. 3). Roberts Mountains allochthon strata are highly deformed, and include imbricated older-over-younger thrust sheets (Evans and Theodore, 1978; Oldow, 1984; Noble and Finney, 1999). The metamorphic grade of the strata is generally greenschist facies or lower (Gehrels et al., 2000a). The RMA was emplaced along the Roberts Mountains thrust during the Late Devonian to Early Mississippian Antler orogeny (Roberts et al., 1958). The Antler foreland basin, west of the Laurentian craton and east of the Antler orogen, was filled between Devonian and Early Mississippian time by sediments shed from the uplifting Antler highlands (Poole, 1974; Trexler et al., 2003) (Fig. 2).

The plate tectonic setting of the Antler orogeny has been variously interpreted as continent-continent collision, continent-arc collision, backarc thrusting, and polarity reversal of a subduction zone (e.g., Nilsen and Stewart, 1980; Speed and Sleep, 1982; Dickinson et al., 1983). The RMA is often interpreted as an accretionary prism formed due to plate convergence at the continental margin (Speed and Sleep, 1982; Oldow, 1984; Dickinson, 2000).

Evidence for Antler-age tectonism has been reported along the western Laurentian margin, in Alaska and Canada (e.g., Nilsen and Stewart, 1980; Gehrels and Smith, 1987; Dusel-Bacon et al., 2006; Nelson et al., 2006; Paradis et al., 2006; Piercey et al., 2006; Colpron et al., 2007). Middle to Late Devonian continental arc magmatism occurred in the Alaska Range and central Yukon (Piercey et al., 2006) (Fig. 1). Upper Devonian–Early Mississippian felsic igneous and metaigneous rocks record bimodal volcanism in east-central Alaska and the Yukon (Dusel-Bacon et al., 2006) (Fig. 1). In south-central British Columbia (Fig. 1), a Late Devonian continental arc and backarc developed (Paradis et al., 2006).

Colpron et al. (2007) and Colpron and Nelson (2009) have proposed a direct link between the Antler orogeny and coeval tectonism of western Laurentia. They propose that a "Northwest Passage" opened in mid-Paleozoic time between Laurentia and Siberia, and a Scotia-style arc developed along the northern Laurentian margin in the Early Devonian (Fig. 3). The Alexander terrane, and other fragments such as the eastern Klamath and northern Sierran terranes, were transported from a Baltica origin to northwestern Laurentia through the Northwest Passage via the westward migration of the arc's subduction zone (Fig. 3). By Middle Devonian time, a sinistral transform fault developed at the southern end of this passage and extended southward along western Laurentia. This system transported these terranes and fragments south along the margin. Colpron and Nelson (2009) note progressively younger deformation southward along the Laurentian margin, from Alaska and the Yukon to Nevada, and suggest that this records the southward propagation of the transpressional system. They propose that this fault system could have provided the weakness along which Devonian subduction initiated.

Roberts Mountains Allochthon Strata

The RMA strata sampled (Figs. 2 and 4; Table 1) are arenite beds within units that are predominantly chert and argillite with some limestone and mafic volcanic rocks. Most contacts between and within units are structural, and the stratigraphic bases and tops of units are not known. The strata of the RMA are described briefly below, as evidence of their depositional environments.

The Snow Canyon Formation and the McAfee Quartzite in the Independence Mountains (Figs. 2 and 4; Table 1) are the equivalent of the upper Vinini and Valmy formations, respectively (Holm-Denoma et al., 2011). Both units are Middle Ordovician based on graptolite fauna (Churkin and Kay, 1967). The Snow Canyon Formation is predominantly chert with arenite, shale, and siltstone layers, and basaltic lavas with interbedded limestone (Churkin and Kay, 1967). The McAfee Quartzite is predominantly massive cliff-forming quartzite with intervals of shale and siltstone and bedded chert (Churkin and Kay, 1967). The arenite intervals in these formations are interpreted as turbidites (Miller and Larue, 1983).

The Vinini Formation (Figs. 2 and 4; Table 1) was first mapped in the Roberts Mountains by Merriam and Anderson (1942) along Vinini Creek. Merriam and Anderson (1942) recognized two informal units (upper and lower) based on lithology and graptolite fauna and described the extreme structural disruption of these rocks. In later work, Noble and Finney (1999) used precise radiolarian biostratigraphy to demonstrate a high degree of structural imbrication both within the Vinini Formation and within Devonian cherts. In the Toquima Range, near Petes Summit (Fig. 2), the Vinini Formation is divided into two informal units (upper and lower), which are mapped in depositional contact, and the extreme structural complexity and repetition of thrust slices is also mapped (McKee, 1976). We observed the depositional contact at Petes Summit, where the quartz arenite of the upper Vinini rests on shale of the lower Vinini. The lower Vinini Formation is predominantly quartz arenite, with siltstone, shale, chert, and limestone (Finney et al., 1993). The lower Vinini Formation is Upper Lower to Lower Middle Ordovician in age, based on graptolite and conodont fauna (Finney et al., 1993). The arenite intervals in the lower Vinini Formation are interpreted as turbidites (Finney et al., 1993). The upper Vinini Formation is predominantly shale and bedded chert, with some siltstone and arenite (Finney et al., 1993). The unit is Middle Middle to Upper Ordovician, based on graptolites and conodonts (Finney et al., 1993). Graptolites and conodonts of the lower Vinini Formation are similar to those found in coeval Laurentian shelf carbonate deposits (Finney and Ethington, 1992; Finney, 1998). At Petes Summit, we observed low-angle cross lamination and hummocky cross stratification in the arenite of the upper Vinini Formation. We therefore interpret the upper Vinini as having been deposited in a high-energy environment at a depth above storm wave base on the continental shelf and probably at less than 100 m depth.

The Elder Sandstone (Figs. 2 and 4; Table 1) is predominantly fine-grained sandstone and siltstone, with some cherty shale and quartzite (Gilluly and Gates, 1965). Fossils are sparse in the unit; the age is Lower Silurian based on graptolites (Gilluly and Gates, 1965). The Elder Sandstone is interpreted as a turbidite deposit (Madrid, 1987).

The Slaven Chert (Figs. 2 and 4; Table 1) is predominantly black, bedded chert with shale beds and some limey sandstone and siltstone (Gilluly and Gates, 1965). The unit is Middle Devonian based on a variety of fossils (Gilluly and Gates, 1965). The arenite intervals in the Slaven Chert are interpreted as turbidites (Madrid, 1987).

METHODS

Zircon grains from six arenite samples were analyzed for U-Pb ages and Hf isotope ratios (Figs. 2 and 4; Table 1). A small number of zircon grains from these samples were previously analyzed for U-Pb ages by Gehrels et al. (2000a), using

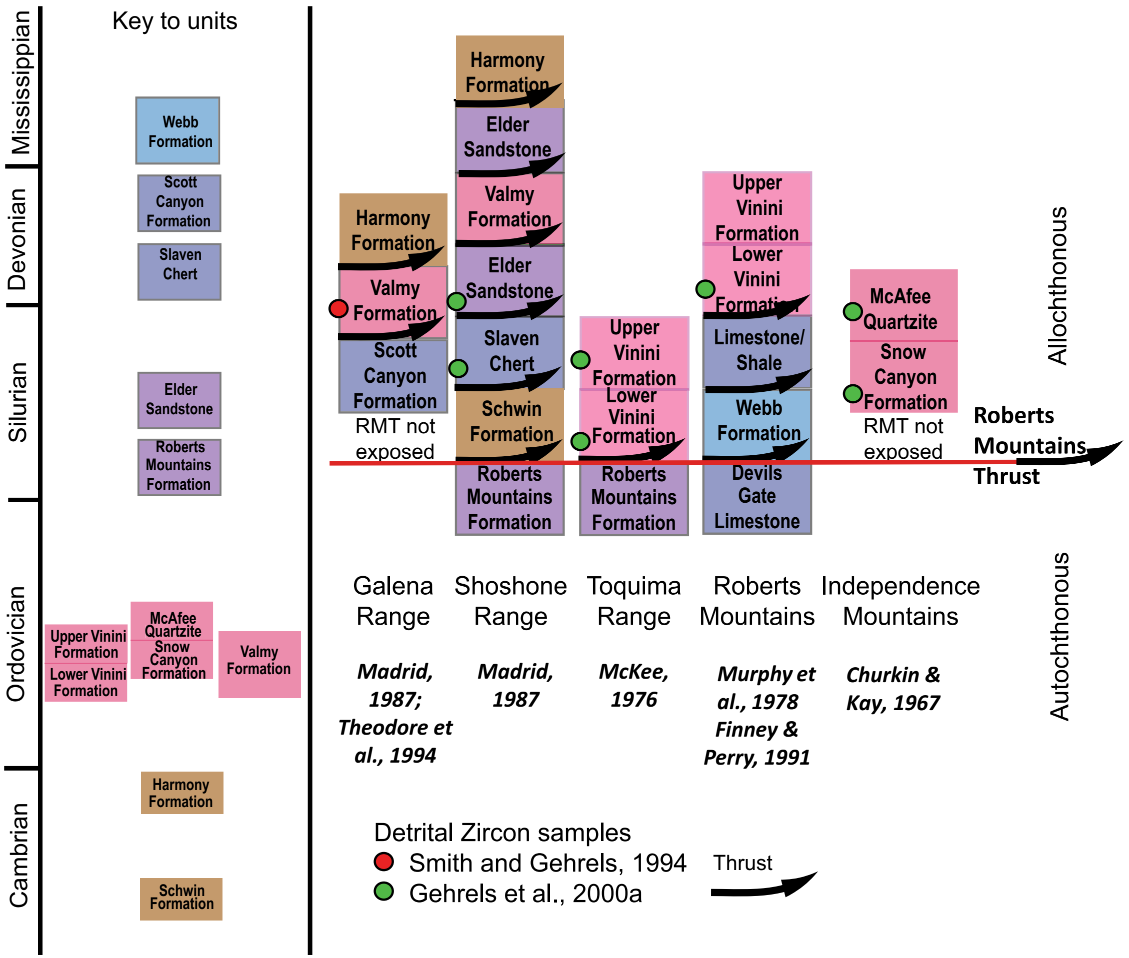

Figure 4. Tectonostratigraphic diagram of units of the Roberts Mountains allochthon (RMA) in selected north-central Nevada mountain ranges, showing locations of detrital zircon samples. Units are shown in their physical, structurally superimposed, order. Most units are internally disrupted with multiple imbricate thrusts not shown on this chart. Units are color coded for geologic period as indicated on left margin of chart.

ID-TIMS (Fig. 5). Zircon grains were separated and analyzed at the University of Arizona LaserChron facility using standard techniques described by Gehrels and Pecha (2014) to yield a best age distribution reflective of the true distribution of detrital zircon ages in each sample. Approximately 200 randomly selected grains were analyzed in each sample for U-Pb ages. Approximately 50 of these grains were subsequently analyzed for Hf isotopes. Hf analyses were conducted on top of the pits left after U-Pb analysis, to ensure that Hf isotope data were collected from the same domain as the U-Pb age. Analyses were conducted by LA-ICPMS using the Photon Machines Anlyte G2 excimer laser connected to the Nu Plasma high-resolution inductively coupled plasma-mass spectrometer, using methods identical to those described by Gehrels and Pecha (2014).

Uranium-Lead Geochronology

Analytical results are displayed graphically on normalized probability plots (Figs. 5 and 6), which allow visual comparison between zircon populations. U-Pb geochronology results are displayed in Figure 5, which contains both data from the original ID-TIMS analyses of these samples (Gehrels et al., 2000a) and the LA-ICPMS analyses of the current study, and in Figure 6, which displays the U-Pb results and Hf isotope analyses of the current study on the same chart. The essential U-Pb isotope information and ages are reported in Supplemental Table 1[1].

We compared detrital zircon age distributions both visually and statistically. Our initial appraisal was visual comparison of the probability plots. We also com-

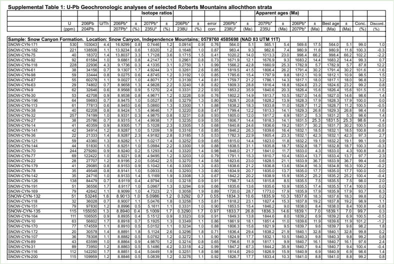

---

[1] Supplemental Table 1. U-Pb geochronologic analyses of selected Roberts Mountains allochthon strata. Please visit http://dx.doi.org/10.1130/GES01252.S1 or the full-text article on www.gsapubs.org to view Supplemental Table 1.

TABLE 1. LOCATIONS OF SAMPLES ANALYZED IN THIS STUDY REFERENCED TO UTM LOCATIONS

Sample Location (UTM: NAD 83)	Easting	Northing
Ordovician Snow Canyon Formation Snow Canyon; Independence Mountains	0579760	4585698 *(UTM 11T)*
Ordovician lower Vinini Formation Petes Summit; Toquima Range	0518089	4337111 *(UTM 11S)*
Ordovician McAfee Quartzite McAfee Peak; Independence Mountains	0590637	4599583 *(UTM 11T)*
Ordovician upper Vinini Formation Petes Summit; Toquima Range	0518089	4337111 *(UTM 11S)*
Silurian Elder Sandstone Elder Creek; Shoshone Range	0516196	4460270 *(UTM 11T)*
Devonian Slaven Chert Slaven Canyon; Shoshone Range	0519428	4479302 *(UTM 11T)*

pared age distributions using the Kolmogorov-Smirnov (K-S) statistic (Guynn and Gehrels, 2006) (Table 2). The K-S statistic calculates whether a statistically significant difference exists between two distributions. $P<0.05$ indicates >95% probability that two U-Pb distributions are not the same. The K-S statistic is sensitive to proportions of ages present, and a low-P value may indicate that the proportions of age peaks are different, even though the ages are similar (Gehrels, 2012).

Hafnium Isotope Analysis

Hafnium isotope data are shown on Hf-evolution diagrams (Fig. 6) that display epsilon $Hf_{(t)}$ ($\varepsilon Hf_{(t)}$) values at the time of crystallization. The essential Hf isotope information is reported in Supplemental Table 2[2].

RESULTS: URANIUM-LEAD AGES AND HAFNIUM ISOTOPE RATIOS

Although the ID-TIMS data (Gehrels et al., 2000a) are similar to the new LA-ICPMS data (Fig. 5), there are variations in the proportions of age groups. The two studies used different grain-selection procedures. For the ID-TIMS study, zircon crystals were selected from color and morphology groups, without regard to the number of grains in each group. For our LA-ICPMS study, we attempted to select grains at random from the entire population of grains. This procedure resulted in a more representative age distribution because the grains are chosen randomly. The results and interpretations that follow are all based upon LA-ICPMS ages from our current study.

Uranium-Lead Ages and Hafnium Isotope Analyses

U-Pb geochronology and Hf isotope analyses reveal that the RMA strata are in two distinct groups. Five of the six samples (the Snow Canyon Formation, the McAfee Quartzite, the upper Vinini Formation, the Elder Sandstone, and the Slaven Chert) yield similar U-Pb age spectra, while the remaining sample, the lower Vinini Formation, yields significantly different U-Pb age spectra (Figs. 5 and 6). The Hf data from the five samples with similar U-Pb ages are similar, while the lower Vinini Formation sample, because of its different age spectra, yields significantly different Hf ratios (Fig. 6).

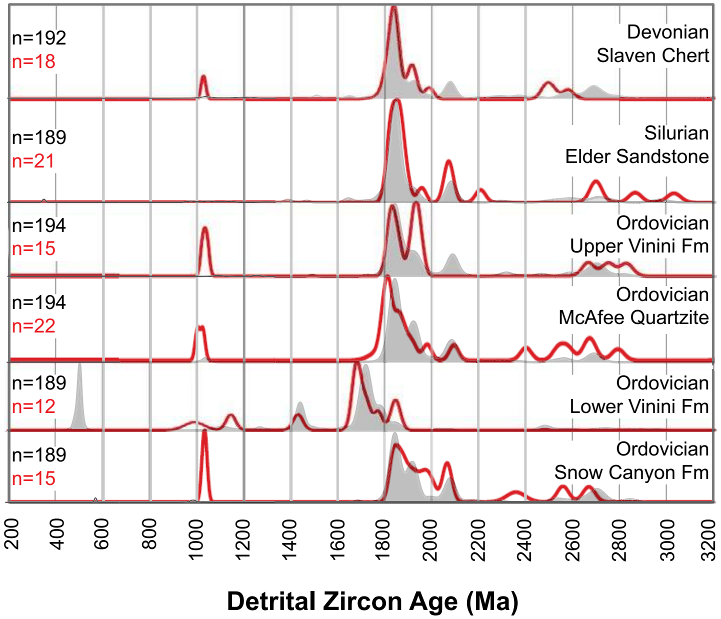

Figure 5. Normalized probability plots showing U-Pb ages of strata sampled. Red lines show the data from isotope-dilution thermal ionization mass spectrometry (Gehrels et al., 2000a); gray-filled curves are the data from laser-ablation inductively coupled plasma mass spectrometry (this study). Numbers of grains analyzed are shown (n =).

PROVENANCE OF THE ROBERTS MOUNTAINS ALLOCHTHON

To interpret provenance, we compared the data from our study to known U-Pb ages and Hf isotope data from Laurentian basement provinces and other sedimentary units.

Provenance of the Roberts Mountains Allochthon Exclusive of the Lower Vinini

The detrital zircon age spectra of the Snow Canyon Formation, the McAfee Quartzite, the upper Vinini Formation, the Elder Sandstone, and the Slaven Chert are consistent with provenance in the Peace River Arch (PRA) region of western Canada (Fig. 7). The 1820–1960 Ma grains are similar in age to magmatic arcs in the PRA region, including the Fort Simpson, the Rimbey, the

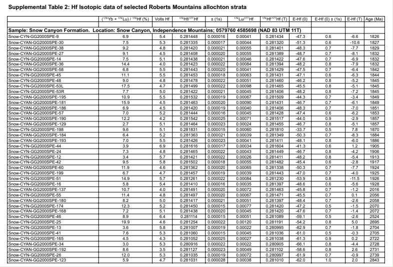

Supplemental Table 2: Hf Isotopic data of selected Roberts Mountains allochton strata

	(^{176}Yb + ^{176}Lu) / ^{176}Hf (%)	Volts Hf	^{176}Hf/^{177}Hf	± (1s)	^{176}Lu/^{177}Hf	^{176}Hf/^{177}Hf (T)	E-Hf (0)	E-Hf (0) ± (1s)	E-Hf (T)	Age (Ma)
Sample: Snow Canyon Formation. Location: Snow Canyon, Independence Mountains; 0579760 4585698 (NAD 83 UTM 11T)										
Snow-CYN-GG2000SPE-9	6.9	5.4	0.281448	0.000016	0.00041	0.281434	-47.3	0.6	-6.6	1826
Snow-CYAN-GG2000SPE-30	7.5	5.3	0.281335	0.000017	0.00044	0.281320	-51.3	0.6	-10.6	1827
Snow-CYAN-GG2000SPE-38	9.2	4.8	0.281420	0.000021	0.00055	0.281401	-48.3	0.7	-7.7	1829
Snow-CYAN-GG2000SPE-27	9.1	4.5	0.281408	0.000020	0.00055	0.281389	-48.7	0.7	-8.1	1832
Snow-CYN-GG2000SPE-14	7.5	5.1	0.281438	0.000021	0.00046	0.281422	-47.6	0.7	-6.9	1832
Snow-CYAN-GG2000SPE-36	14.4	4.0	0.281423	0.000022	0.00084	0.281394	-48.2	0.8	-7.9	1832
Snow-CYAN-GG2000SPE-58	6.8	5.5	0.281443	0.000020	0.00041	0.281429	-47.5	0.7	-6.4	1842
Snow-CYN-GG2000SPE-45	11.1	5.5	0.281453	0.000018	0.00063	0.281431	-47.1	0.6	-6.3	1844
Snow-CYN-GG2000SPE-48	9.0	4.8	0.281478	0.000022	0.00051	0.281460	-46.2	0.8	-5.2	1845
Snow-CYN-GG2000SPE-53L	17.5	4.7	0.281499	0.000022	0.00098	0.281465	-45.5	0.8	-5.1	1845
Snow-CYN-GG2000SPE-53R	7.7	5.0	0.281422	0.000021	0.00045	0.281406	-48.2	0.8	-7.2	1845
Snow-CYAN-GG2000SPE-195	10.9	5.5	0.281532	0.000019	0.00067	0.281509	-44.3	0.7	-3.4	1849
Snow-CYAN-GG2000SPE-181	15.9	4.5	0.281463	0.000020	0.00090	0.281431	-46.7	0.7	-6.1	1849
Snow-CYAN-GG2000SPE-186	6.9	4.5	0.281420	0.000019	0.00040	0.281406	-48.3	0.7	-7.0	1851
Snow-CYAN-GG2000SPE-57	7.0	5.2	0.281444	0.000016	0.00045	0.281428	-47.4	0.6	-6.2	1853
Snow-CYAN-GG2000SPE-190	12.2	4.2	0.281542	0.000025	0.00071	0.281517	-44.0	0.9	-2.9	1857
Snow-CYAN-GG2000SPE-129	2.7	5.1	0.281464	0.000023	0.00024	0.281455	-46.7	0.8	-5.1	1857
Snow-CYN-GG2000SPE-198	9.6	5.1	0.281831	0.000015	0.00060	0.281810	-33.7	0.5	7.8	1870
Snow-CYAN-GG2000SPE-184	6.4	5.2	0.281363	0.000021	0.00039	0.281349	-50.3	0.7	-8.3	1884
Snow-CYAN-GG2000SPE-193	7.0	5.5	0.281426	0.000023	0.00041	0.281411	-48.1	0.8	-6.0	1886
Snow-CYN-GG2000SPE-44	3.9	6.9	0.281616	0.000017	0.00034	0.281604	-41.3	0.6	1.2	1905
Snow-CYN-GG2000SPE-24	7.3	4.8	0.281465	0.000022	0.00043	0.281449	-46.7	0.8	-4.2	1906
Snow-CYN-GG2000SPE-12	3.4	5.7	0.281421	0.000022	0.00026	0.281411	-48.2	0.8	-5.4	1913
Snow-CYN-GG2000SPE-42	9.5	5.8	0.281502	0.000018	0.00055	0.281482	-45.4	0.6	-2.8	1917
Snow-CYAN-GG2000SPE-60	11.9	4.6	0.281362	0.000020	0.00065	0.281338	-50.3	0.7	-7.7	1924
Snow-CYN-GG2000SPE-199	6.7	4.7	0.281457	0.000019	0.00039	0.281443	-47.0	0.7	-4.0	1925
Snow-CYN-GG2000SPE-51	14.9	5.7	0.281261	0.000022	0.00084	0.281230	-53.9	0.8	-11.5	1926
Snow-CYN-GG2000SPE-16	5.8	5.4	0.281410	0.000016	0.00035	0.281397	-48.6	0.6	-5.6	1928
Snow-CYAN-GG2000SPE-137	10.7	4.0	0.281491	0.000020	0.00072	0.281463	-45.8	0.7	-1.2	2016
Snow-CYN-GG2000SPE-55	11.4	4.8	0.281497	0.000020	0.00067	0.281471	-45.5	0.7	0.1	2056
Snow-CYAN-GG2000SPE-180	8.2	5.0	0.281417	0.000021	0.00051	0.281397	-48.4	0.7	-2.6	2058
Snow-CYN-GG2000SPE-174	12.3	5.2	0.281450	0.000015	0.00077	0.281420	-47.2	0.5	-1.5	2070
Snow-CYAN-GG2000SPE-168	7.2	5.1	0.281438	0.000020	0.00045	0.281420	-47.6	0.7	-1.4	2072
Snow-CYN-GG2000SPE-46	8.9	6.4	0.281114	0.000015	0.00051	0.281089	-59.1	0.5	-2.6	2524
Snow-CYN-GG2000SPE-25	19.9	4.6	0.281254	0.000022	0.00120	0.281191	-54.2	0.8	5.0	2695
Snow-CYN-GG2000SPE-13	3.6	5.8	0.281007	0.000019	0.00022	0.280995	-62.9	0.7	-1.8	2704
Snow-CYN-GG2000SPE-41	7.6	5.3	0.281060	0.000015	0.00045	0.281036	-61.0	0.5	-0.3	2705
Snow-CYN-GG2000SPE-165	4.5	4.3	0.281052	0.000025	0.00027	0.281038	-61.3	0.9	0.2	2722
Snow-CYAN-GG2000SPE-34	3.0	5.3	0.280916	0.000022	0.00022	0.280905	-66.1	0.8	-4.4	2728
Snow-CYAN-GG2000SPE-192	8.6	3.5	0.281127	0.000023	0.00049	0.281102	-58.6	0.8	2.6	2731
Snow-CYN-GG2000SPE-26	12.0	5.3	0.281035	0.000019	0.00072	0.280997	-61.9	0.7	-0.9	2739
Snow-CYAN-GG2000SPE-123	5.9	4.7	0.281031	0.000028	0.00038	0.281010	-62.0	1.0	2.0	2843

---

[2] Supplemental Table 2. Hf isotope data of selected Roberts Mountains allochthon strata. Please visit http://dx.doi.org/10.1130/GES01252.S2 or the full-text article on www.gsapubs.org to view Supplemental Table 2.

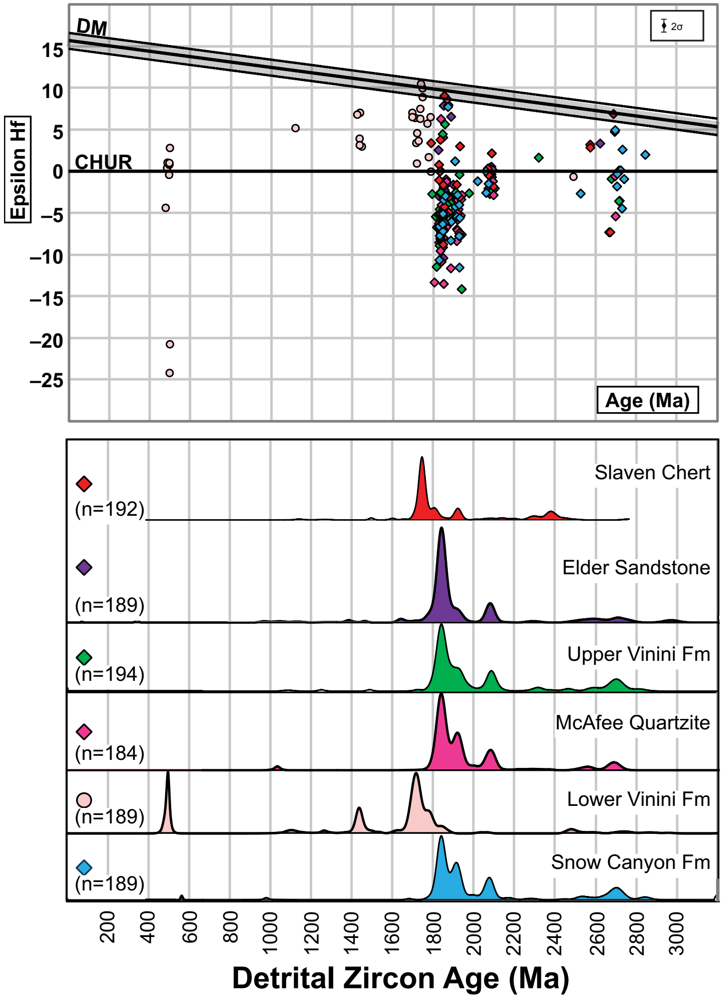

Figure 6. U-Pb ages and Hf isotope data for Roberts Mountains allochthon strata. U-Pb dates were run for all sample grains; approximately one-fourth of these grains were analyzed for hafnium isotopes. The upper graph shows $\varepsilon Hf_{(t)}$ (epsilon Hf) values for each sample. The average measurement uncertainty for all hafnium analyses is shown in the upper right at the 2σ of the values. Reference lines on the Hf plot are as follows: Depleted mantle (DM) is calculated using $^{176}Hf/^{177}Hf$ = 0.283225; $^{176}Lu/^{177}Hf$ = 0.038513 (Vervoort and Blichert-Toft, 1999); CHUR—chondritic uniform reservoir, is calculated using $^{176}Hf/^{177}Hf$ = 0.282785 and $^{176}Lu/^{177}Hf$ = 0.0336 (Bouvier et al., 2008).

Ksituan, and the Great Bear arcs (Hoffman, 1989; Ross, 1991; Villeneuve et al., 1993) (Fig. 7). The 2060–2120 Ma grains are similar in age to accreted terranes in the PRA region, including the Buffalo Head and Chincaga terranes (Hoffman, 1989; Ross, 1991; Villeneuve et al., 1993) (Fig. 7). The 2650–2750 Ma grains are similar in age to Archean terranes in the PRA region, including the Nova and Hearne terranes (Hoffman, 1989; Ross, 1991; Villeneuve et al., 1993) (Fig. 7).

The Hf isotope data are consistent with provenance in the PRA region. The 1820–1960 Ma grains have a wide range of values, from juvenile and moderately juvenile through evolved ($\varepsilon Hf_{(t)}$ +10 to –15), similar to those of other units interpreted to originate in the PRA region (Gehrels and Pecha, 2014). The 2060–2120 Ma grains are more narrowly grouped, with moderately juvenile to evolved values of $\varepsilon Hf_{(t)}$ +3 to –6, compatible with other units originating in the PRA region (Gehrels and Pecha, 2014). The 2560–2750 Ma grains have juvenile, moderately juvenile, and evolved values of $\varepsilon Hf_{(t)}$ +6 to –15, also compatible with PRA origin (Gehrels and Pecha, 2014). The ages of basement terranes that comprise the PRA region (Fig. 7) are all represented in the age spectra of the RMA samples (exclusive of the lower Vinini Formation).

The detrital zircon U-Pb ages and Hf isotope data from these RMA strata are similar to selected passive margin strata and RMA strata analyzed in other studies (Fig. 8). The RMA strata sampled in this study (exclusive of the lower Vinini) have U-Pb age spectra similar to those of the Ordovician Valmy Formation of the RMA (Gehrels and Pecha, 2014), as well as the Eureka Quartzite and the Mount Wilson Formation (Gehrels and Pecha, 2014), and the Kinnikinic Quartzite (Barr, 2009), Ordovician units of the western Laurentian passive margin (Figs. 8 and 9). The K-S analyses of the RMA and the Ordovician passive margin units discussed above do not contradict our interpretation that the RMA strata have a common provenance with the Ordovician passive margin sandstones (Table 2). These RMA strata also show similar Hf isotope ratios to the Valmy Formation (Gehrels and Pecha, 2014) and to the Eureka Quartzite and the Mount Wilson Formation (Gehrels and Pecha, 2014) (Fig. 8).

The Peace River Arch region of western Canada is the source for the RMA units in this study, exclusive of the lower Vinini Formation, and for the Ordovician passive margin sandstones. The Peace River Arch region was an uplifted region from late Neoproterozoic through Middle Devonian time (Cant, 1988; Cant and O'Connell, 1988; Cecile et al., 1997). Igneous bodies in the PRA region have ages similar to the U-Pb ages of zircons in the RMA rocks sampled (Figs. 7 and 8). The U-Pb age spectra of the RMA rocks sampled are not consistent with derivation from the central Laurentian craton; the Yavapai-Mazatzal terranes are 1.6–1.8 Ga and cannot serve as a source of the 1.8–2.0 Ga grains in the samples.

Provenance of the Lower Vinini Formation

The U-P age spectra of the lower Vinini Formation are consistent with provenance in north-central Laurentia. The 490–500 Ma grains are similar in age to plutonic suites in roof pendants and inliers within the Challis volcanic-plutonic complex and the Idaho batholith (Lund et al., 2010). The 1110–1120 Ma grains are consistent with the Grenville orogen; the 1420 Ma grains are consistent with the central Laurentian anorogenic granites; the 1660–1800 Ma grains are consistent with the Yavapai-Mazatzal terranes; and the 2470–2750 Ma grains

TABLE 2. K-S STATISTICAL ANALYSIS RESULTS

	Slaven Chert	Elder Sandstone	Valmy Formation	Upper Vinini Formation	McAfee Quartzite	Snow Canyon Formation	Eureka Quartzite	Kinnikinic Quartzite	Mount Wilson Formation
Slaven Chert		0.130	0.156	0.402	0.103	0.069	0.064	0.239	0.010
Elder Sandstone	0.130		0.001	0.001	0.013	0.000	0.000	0.000	0.000
Valmy Formation	0.156	0.001		0.330	0.018	0.458	0.118	0.010	0.050
Upper Vinini Formation	0.402	0.001	0.330		0.203	0.872	0.748	0.307	0.348
McAfee Quartzite	0.103	0.013	0.018	0.203		0.318	0.433	0.990	0.020
Snow Canyon Formation	0.069	0.000	0.458	0.872	0.318		0.786	0.313	0.200
Eureka Quartzite	0.064	0.000	0.118	0.748	0.433	0.786		0.948	0.768
Kinnikinic Quartzite	0.239	0.000	0.010	0.307	0.990	0.313	0.948		0.104
Mount Wilson Formation	0.010	0.000	0.050	0.348	0.020	0.200	0.768	0.104	

Note: The Roberts Mountains allochthon (RMA) strata are shown with green highlights, and the passive margin strata are shown with blue highlights. Comparisons between units with values greater than 0.05 are highlighted in yellow. P<0.05 indicates >95% probability that two U-Pb distributions are not the same. K-S—Kolmogorov-Smirnov.

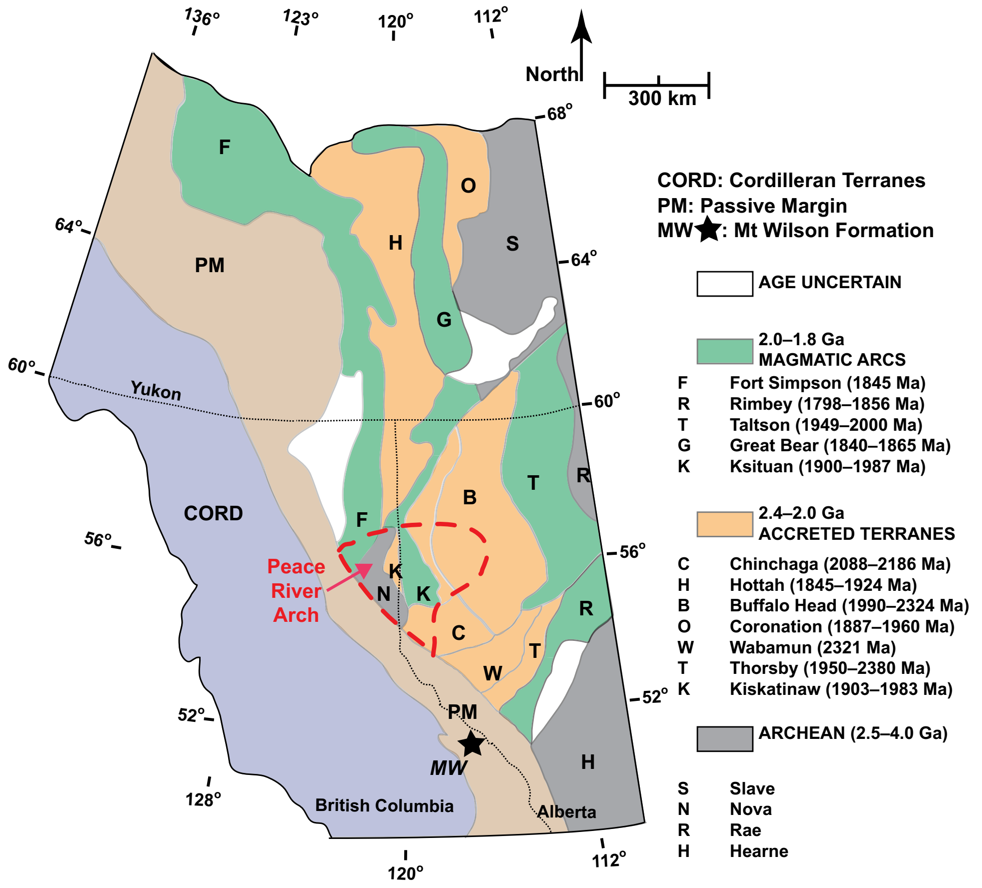

Figure 7. Map of western Canada showing the Cordilleran accreted terranes, the Cordilleran passive margin, and the basement provinces of the Canadian Shield. The Peace River Arch region is outlined by the red dashed line. The location of the Mount Wilson Formation sample (Gehrels and Pecha, 2014) is shown. The map is after Gehrels and Ross (1998); the basement provinces are compiled from Hoffman (1989), Ross (1991), and Villeneuve et al. (1993). WY—Wyoming province; HE—Hearn province; SU—Superior province; CORD—Cordilleran; APP—Appalachian; OA—Ouachita-Marathon; MOJ—Mojavia.

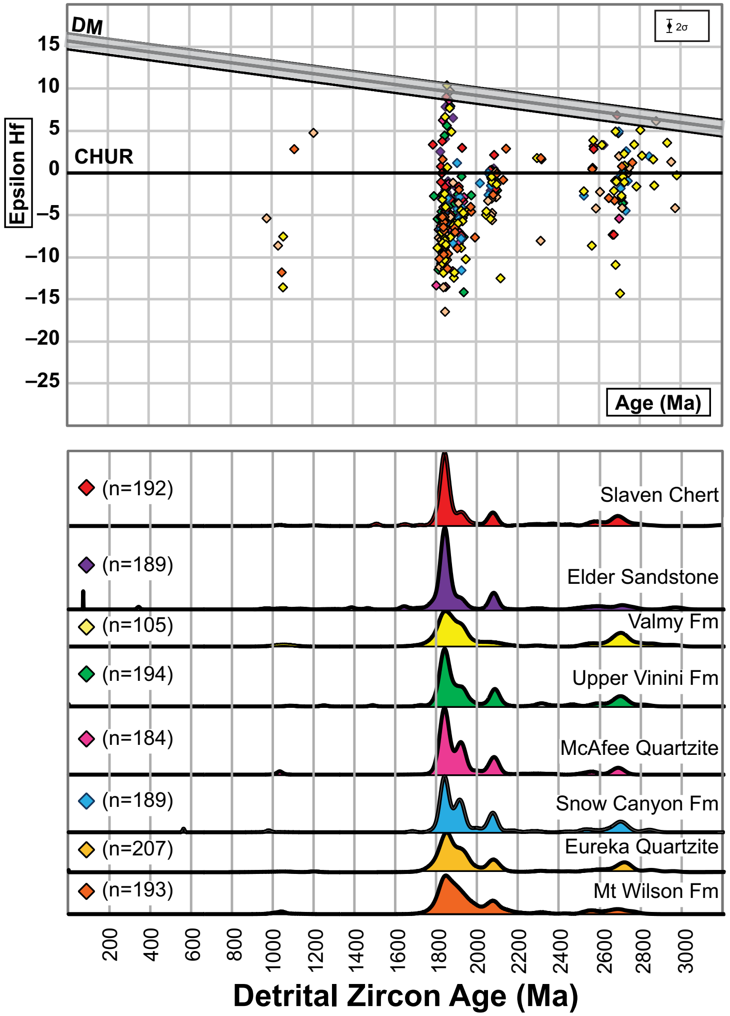

Figure 8. U-Pb ages and Hf isotope data. The data from the Mount Wilson Formation, the Eureka Quartzite, and the Valmy Formation are from Gehrels and Pecha (2014). Diagrams and symbols are as in Figure 4.

are consistent with the Archean craton (Bickford et al., 1986; Hoffman, 1989; Ross, 1991; Anderson and Morrison, 1992; Bickford and Anderson, 1993; Van Schmus et al., 1993) (Fig. 1). River systems traversing the north-central craton from east to west transported sediments from these crystalline bedrock sources—or from sediments recycled from them—and subsequently deposited them off the western Laurentian margin as the lower Vinini Formation.

The Hf isotope data of the lower Vinini grains are also consistent with origin in north-central Laurentia. The 490–500 Ma grains have mostly moderately juvenile to evolved values ($\varepsilon\mathrm{Hf}_{(t)}$ +3 to –5), with two grains highly evolved ($\varepsilon\mathrm{Hf}_{(t)}$ –20 to –25). The moderately juvenile to evolved grains are compatible with the plutonic suites in Idaho; however, the highly evolved grains are unlike any analyzed in these suites (Todt and Link, 2013). The 1110–1120 Ma grains have moderately juvenile values ($\varepsilon\mathrm{Hf}_{(t)}$ +4 to +6), similar to those of the Grenville orogen (Mueller et al., 2008; Bickford et al., 2010). The 1420 Ma grains have juvenile to moderately juvenile values ($\varepsilon\mathrm{Hf}_{(t)}$ +7 to +3), compatible with the anorogenic granitoids of the mid-Laurentian craton (Goodge and Vervoort, 2006). The 1660–1800 Ma grains have juvenile to moderately juvenile values ($\varepsilon\mathrm{Hf}_{(t)}$ +10–0), similar to the Yavapai-Mazatzal terranes (Bickford et al., 2008). The 2470–2750 Ma grains have moderately juvenile to evolved values ($\varepsilon\mathrm{Hf}_{(t)}$ +6 to –6), compatible with those in northern Greenland and Arctic Canada (Rohr et al., 2008, 2010) (Fig. 1).

The Early Cambrian uplift of the Transcontinental Arch altered the drainage patterns in western Laurentia; this change is recorded in the changing detrital zircon age patterns between upper Neoproterozoic and Lower Cambrian passive margin strata (Linde et al., 2014, and references cited therein) (Fig. 10). The uplift of the arch blocked the transport of Grenville-age grains and created, on the west flank of the arch itself, a new highland and source of sand, consisting of Yavapai-Mazatzal basement rocks and sedimentary rocks recycled from this basement. In many older passive margin strata that predate the uplift of the arch, Grenville-age grains predominate (Fig. 10). These grains were transported by continent-spanning rivers that drained the central craton and Grenville orogenic terrane to the western Laurentian margin through the late Neoproterozoic (Rainbird et al., 1997, 2012). In many younger passive margin strata, deposited after the uplift of the arch, Yavapai-Mazatzal–age grains dominate (Fig. 10). Rivers originating in the central craton were blocked from flowing to the west by the uplifted arch, which blocked the transport of many Grenville-age grains (Amato and Mack, 2012; Gehrels and Pecha, 2014; Linde et al., 2014; Yonkee et al., 2014).

The detrital zircon U-Pb ages and Hf isotope data of the lower Vinini Formation resemble those of the younger, post–Transcontinental Arch uplift, passive margin strata, such as the Geersten Quartzite of Utah and the Osgood Mountains Quartzite of Nevada (Fig. 11). These are the only post–arch uplift passive margin data sets for which we have both U-Pb ages and Hf isotope data. The lower Vinini Formation U-Pb age spectra and Hf isotope ratios are similar to those of the younger passive margin strata. The provenance of the lower Vinini Formation is central Laurentian, shed from the western flanks of the Transcontinental Arch and the regions to the west of the arch, after the uplift of the arch (Fig 1).

Discussion: Sedimentology and Paleogeographic Implications

Sedimentological analyses provide a further constraint and suggest that the Ordovician passive margin sandstones are not the source of the RMA strata, but rather that these strata have a common source. Finney and Perry

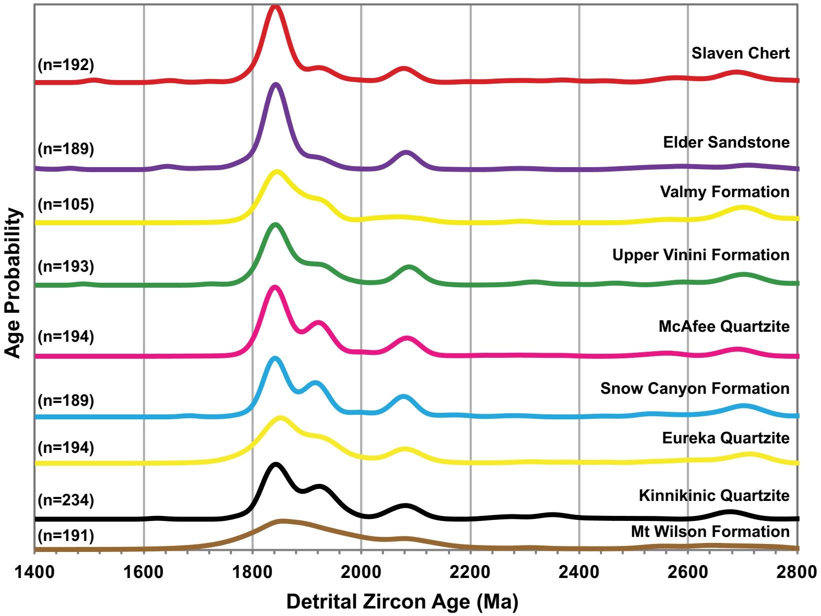

Figure 9. Normalized probability plot of Roberts Mountains allochthon (RMA) strata from this study, exclusive of the lower Vinini Formation. The plot includes the Valmy Formation of the RMA, analyzed by Gehrels and Pecha (2014). The plot also includes select Ordovician passive margin strata: the Mount Wilson Formation and Eureka Quartzite (Gehrels and Pecha, 2014) and the Kinnikinic Quartzite (Barr, 2009). No Hf isotope data are available for the Kinnikinic Quartzite, so only a normalized probability plot is shown.

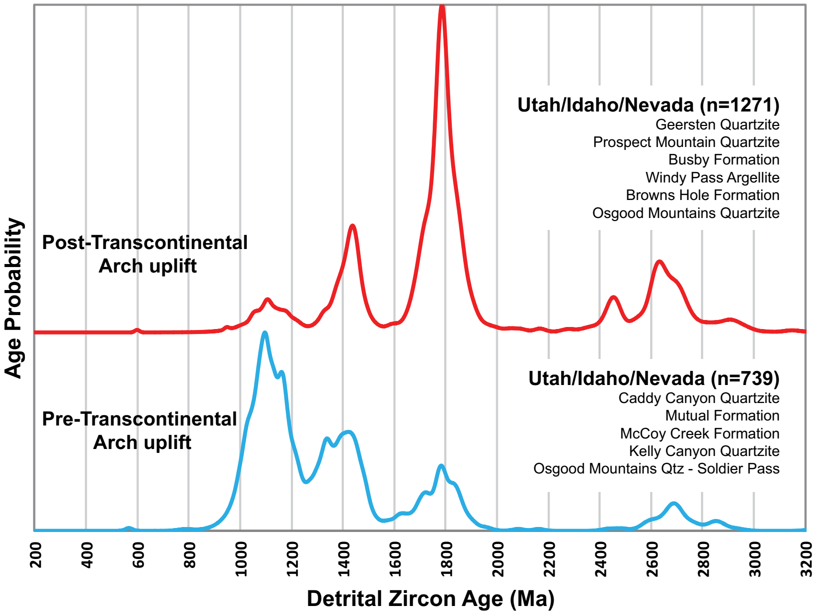

Figure 10. Compilation plots of units showing the distribution of detrital zircon ages in upper Neoproterozoic–Cambrian western Laurentian passive margin units (after Linde et al., 2014). The upper curve (red) is a compilation of ages of the relatively younger strata throughout the region. The lower curve (blue) is a compilation of ages of the relatively older strata throughout the region. The curves are normalized probability plots. The number of detrital zircon grains comprising each compilation is shown on the right. Osgood Mountains Quartzite (Linde et al., 2014); Kelley Canyon Quartzite, Caddy Canyon Quartzite, Brown's Hole Formation, Geersten Canyon Quartzite, Mutual Formation, Prospect Mountain Quartzite, McCoy Creek Group, Busby Formation, and Windy Pass Argillite (Yonkee et al., 2014); Kelley Canyon Quartzite, Caddy Canyon Quartzite, Mutual Formation, and Prospect Mountain Quartzite (Lawton et al., 2010).

Figure 11. U-Pb ages and Hf isotope data for Roberts Mountains allochthon (RMA) and select Laurentian passive margin strata. The data from the Osgood Mountains Quartzite and the Geersten Canyon Quartzite are from Gehrels and Pecha (2014). The lower Vinini data includes those from this study (n = 189) and from Gehrels and Pecha (2014) (n = 105). Diagrams and symbols are as in Figure 5.

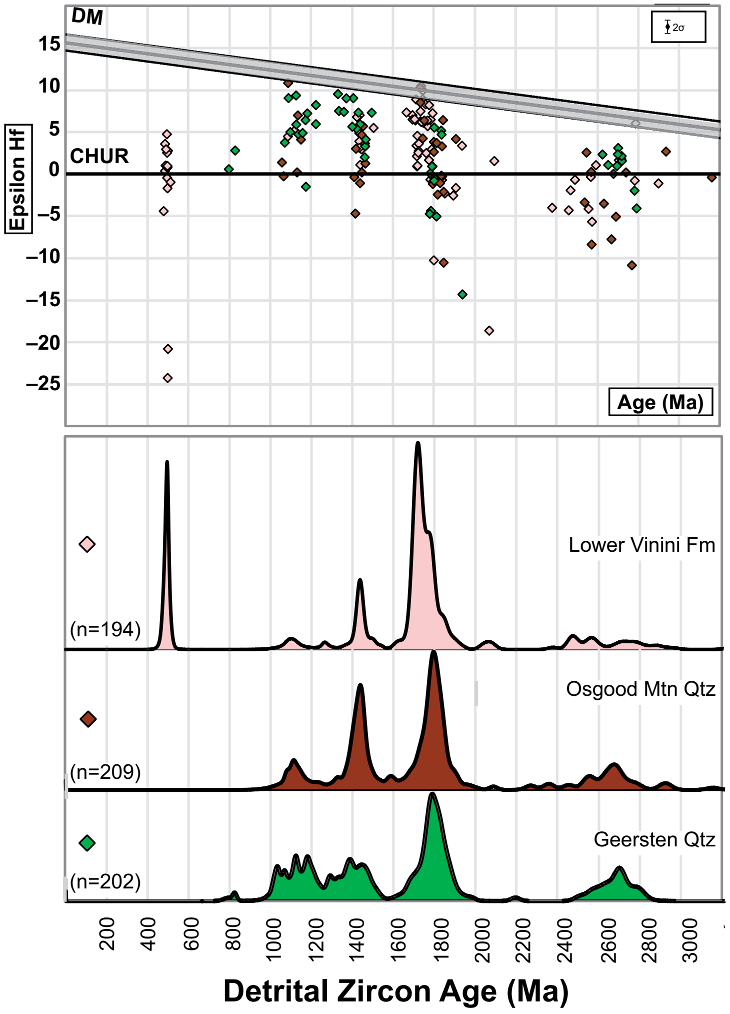

(1991) proposed that the Eureka Quartzite (an extensive Ordovician passive margin unit) was the source of the sandstones in the younger sections of the Vinini and Valmy formations of the RMA. However, the grains of the Ordovician passive margin sandstones are more texturally mature than those of the RMA strata, whose grains are coarser, larger, and more poorly sorted (Ketner, 1966). The more mature shelf sands such as the Eureka Quartzite and Mount Wilson Formation could not be the source of the more immature RMA sandstones. The RMA and passive margin sandstones have similar U-Pb age spectra and Hf isotope ratios (Fig. 7) and share a common source in the PRA region.

The Ordovician passive margin sands and the RMA strata sampled have different depositional histories (Fig. 12). The Mount Wilson Formation was deposited in a nearshore to shelf environment immediately outboard of the Peace River Arch (Kent, 1994). Other Ordovician passive margin sandstones, now preserved as the Eureka Quartzite and the Kinnikinic Quartzite, were shed from the Peace River Arch, and subsequently moved southward along the western Laurentian margin via longshore transport to the depositional basin (Ketner, 1968) (Fig. 12B). The evidence for this transport is that grain size decreases and sorting improves in Ordovician arenites from near the PRA source (the Mount Wilson Formation) southward through Idaho (the Kinnikinic Quartzite) and into Nevada and California (the Eureka Quartzite) (Ketner, 1968). The texturally immature arenites of the RMA did not undergo the extensive reworking of this longshore transport. Sediments of the RMA strata, other than the lower Vinini Formation, were deposited as turbidites (Miller and Larue, 1983; Madrid, 1987; Finney et al., 1993) offshore of the Peace River Arch (Figs. 12A–12C).

To reach their current geographic location, the RMA strata were *tectonically* transported south along the western Laurentian margin, in Latest Devonian time (Fig. 12E). This is consistent with a sinistral transpressional fault system, as proposed by Colpron and Nelson (2009) (Figs. 12D and 12E). Subsequent shortening moved the RMA up onto the craton in the Antler orogeny of Latest Devonian–Earliest Mississippian time (Figs. 12E and 12F).

CONCLUSIONS

These U-Pb geochronology and Hf isotope analyses of RMA strata give new insight into their provenance. We confirmed previous work that had indicated different detrital zircon U-Pb ages among strata of the RMA, implying different sources for these units. New data indicate that provenance of the lower Vinini Formation is north-central Laurentia, shed from the western flanks of the uplifted Transcontinental Arch. Other RMA strata sampled, Ordovician–Devonian, are similar to Ordovician passive margin sandstones that crop out widely through western North America. These units share a common source in the Peace River Arch region.

Combining sedimentology with detrital zircon data reveals the relationship between the RMA strata and passive margin shelf sands, making it possible to distinguish between sedimentary transport and tectonic transport of the RMA strata. The Ordovician passive margin sands were deposited in the PRA region, and some sand was carried south and reworked by longshore transport. In contrast, the Ordovician–Devonian RMA strata (exclusive of the lower

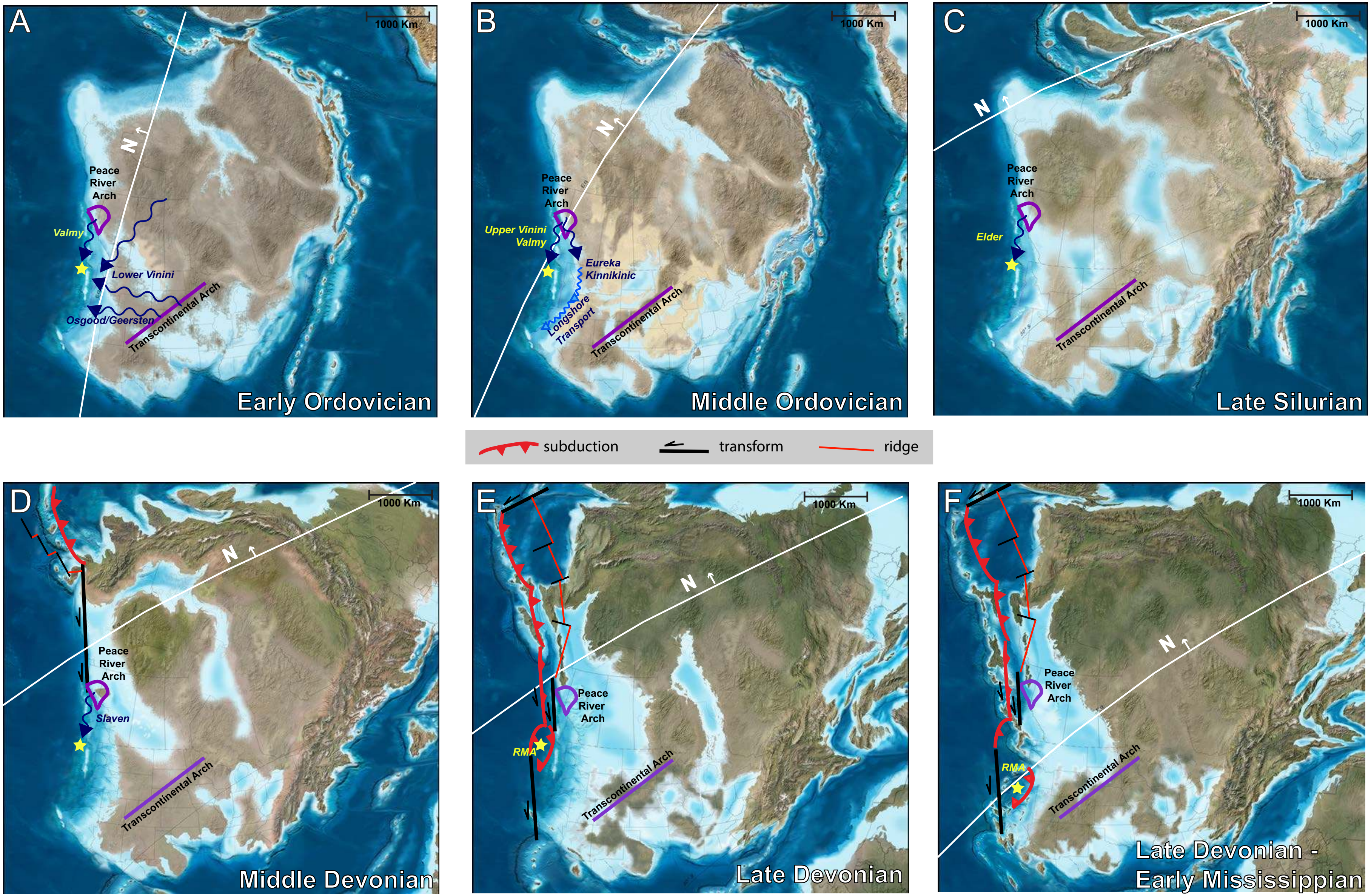

Figure 12. Paleogeographic maps of Laurentia from Middle Ordovician through Mississippian time (Blakey, 2013). Stars represent the depositional basin of Roberts Mountains allochthon (RMA) strata. White lines show the approximate position of the paleoequator. Blue wavy lines show approximate depositional pathways of units discussed. Transcontinental Arch (Sloss, 1988) and Peace River Arch (Ross, 1991) are superimposed. (A) Early Ordovician time. The lower Vinini is derived from the central craton and Transcontinental Arch; the Valmy Formation is derived from the Peace River Arch. (B) Middle Ordovician time. The upper Vinini and Valmy formations are shed from the Peace River Arch into an oceanic basin. The Eureka Quartzite is also derived from the Peace River Arch and transported via longshore current along the western Laurentian margin. (C) Late Silurian time. The Elder Sandstone is shed from the Peace River Arch region. (D) Middle Devonian time. The Slaven Chert is derived from the Peace River Arch. A Scotia-style arc has moved to the western margin of northern Laurentia, and a sinistral transpressional fault system has developed along the western margin. RMA strata are tectonically transported south along the margin by this fault system. (E) Late Devonian time. Subduction has initiated along much of the western margin of Laurentia, moving the RMA strata onto the craton. (F) Early Mississippian time. The Antler orogeny has uplifted the RMA strata into a highland on the western Laurentian margin.

Vinini) were deposited in a shelf, slope, or basin environment offshore of the PRA region; the arenite intervals in these units were deposited as shelf sands or turbidites. These RMA strata, along with the lower Vinini Formation, were tectonically transported in Late Devonian time southward along the margin on a sinistral transpressional fault system. The entire RMA package was subsequently emplaced eastward onto the craton during the Late Devonian–Early Mississippian Antler orogeny.

ACKNOWLEDGMENTS

We would first like to acknowledge the essential role that Bill Dickinson played in all of our RMA studies. Bill was an incomparable mentor and model for all of us and is already sorely missed. *Requiem aeternam dona ei, Domine, et requiescat in pace.*

Additionally, we thank the researchers and staff at the Arizona LaserChron center, especially Mark Pecha and Nicole Giesler and volunteer laboratory assistants Dan Sturmer of Shell Oil Company and University of Nevada, Reno, graduate students Connor Newman and Kyle Basler-Reeder for critical help in Tucson. This research was funded under Arizona LaserChron National Science Foundation (NSF) grant EAR-1338583 to Gehrels. The original collecting effort for these samples was supported by NSF grants EAR-9116000 and EAR-9416933. Linde also thanks the following organizations for generous scholarship support of her graduate work: Raytheon Corporation Student Veterans Scholarship, the Rocky Mountain Association of Geologists Veteran Memorial Scholarship, the Nevada Petroleum and Geothermal Society, the Graduate Student Association of the University of Nevada, Reno, and the Cordilleran Section of the Geological Society of America.

REFERENCES CITED

Amato, J.M., and Mack, G.H., 2012, Detrital zircon geochronology from the Cambrian–Ordovician Bliss Sandstone, New Mexico: Evidence for contrasting Grenville-age and Cambrian sources on opposite sides of the Transcontinental Arch: Geological Society of America Bulletin, v. 124, p. 1826–1840, doi:10.1130/B30657.1.

Anderson, J.L., and Morrison, J., 1992, The role of anorogenic granites in the Proterozoic crustal development of North America, *in* Condie, K.C., ed., Proterozoic Crustal Evolution: New York, Elsevier, p. 263–299.

Bahlburg, H., Vervoort, J.D., DuFrane, S.A., Carlotto, V., Reimann, C., and Cardenas, J., 2011, The U-Pb and Hf isotope evidence of detrital zircons of the Ordovician Ollantaytambo Formation, southern Peru, and the Ordovician provenance and paleogeography of southern Peru and northern Bolivia: Journal of South American Earth Sciences, v. 32, p. 196–209, doi:10.1016/j.jsames.2011.07.002.

Barr, E.E., 2009, Determining the regional-scale detrital zircon provenance of the Middle-Late Ordovician Kinnikinic (Eureka) Quartzite, east-central Idaho, U.S. [M.S. thesis]: Pullman, Washington, Washington State University, 134 p.

Bickford, M.E., and Anderson, J.L., 1993, Middle Proterozoic magmatism, *in* Reed, J.C., Bickford, M.E., Houston, R.S., Link, P.K., Rankin, D.W., Sims, P.K., and Van Schmus, W.R., eds., Precambrian Conterminous U.S.: Boulder, Colorado, Geological Society of America, The Geology of North America, v. C-2, p. 281–292.

Bickford, M.E., Van Schmus, R., and Zietz, I., 1986, Proterozoic history of the midcontinent region of North America: Geology, v. 14, no. 6, p. 492–496, doi:10.1130/0091-7613(1986)14<492:PHOTMR>2.0.CO;2.

Bickford, M.E., Mueller, P.A., Kamenov, G.D., and Hill, B.M., 2008, Crustal evolution of southern Laurentia during the Paleoproterozoic: Insights from zircon isotopic studies of ca. 1.75 Ga rocks in central Colorado: Geology, v. 36, p. 555–558.

Bickford, M.E., McLelland, J.M., Mueller, P.A., Kamenov, G.D., and Neadle, M., 2010, Hafnium isotopic compositions of zircon from Adirondack AMCG suites: Implications for the petrogenesis of anorthosites, gabbros, and granitic members of the suites: Canadian Mineralogist, v. 48, p. 751–761, doi:10.3749/canmin.48.2.751.

Blakey, R., 2013, Key Time Slices of North American Geologic History: cpgeosystems.com/nam.html.

Bouvier, A., Vervoort, J.D., and Patchett, J.D., 2008, The Lu-Hf and Sm-Nd isotopic composition of CHUR: Constraints from unequilibrated chondrites and implications for the bulk composition of terrestrial planets: Earth and Planetary Science Letters, v. 273, p. 48–57, doi:10.1016/j.epsl.2008.06.010.

Burchfiel, B.C., and Davis, G.A., 1972, Structural framework and evolution of the southern part of the Cordilleran orogen, western United States: American Journal of Science, v. 272, p. 97–118, doi:10.2475/ajs.272.2.97.

Burchfiel, B.C., Cowan, D.S., and Davis, G.A., 1992, Tectonic overview of the Cordilleran orogen in the western United States, *in* Burchfiel, B.C., Lipman, P.W., and Zoback, M.L., eds., The Cordilleran orogen: Conterminous U.S.: Boulder, Colorado, Geological Society of America, The Geology of North America, v. G-3, p. 407–480.

Cant, D.J., 1988, Regional structure and development of the Peace River Arch, Alberta: A Paleozoic failed-rift system?: Bulletin of Canadian Petroleum Geology, v. 36, p. 284–295.

Cant, D., and O'Connell, S., 1988, The Peace River Arch: Its structure and origin, *in* James, D.P., and Leckie, D.A., eds., Sequences, Stratigraphy, Sedimentology: Surface and Subsurface: Canadian Society of Petroleum Geologists, Memoir 15, p. 537–542.

Cecile, M.P., Morrow, D.W., and Williams, G.K., 1997, Early Paleozoic (Cambrian to Early Devonian) tectonic framework, Canadian Cordillera: Bulletin of Canadian Petroleum Geology, v. 45, p. 54–74.

Churkin, M., Jr., and Kay, M., 1967, Graptolite-bearing Ordovician siliceous and volcanic rocks, northern Independence Range, Nevada: Geological Society of America Bulletin, v. 78, p. 651–668, doi:10.1130/0016-7606(1967)78[651:GOSAVR]2.0.CO;2.

Colpron, M., and Nelson, J., 2009, A Palaeozoic Northwest Passage: Incursion of Caledonian, Baltican and Siberian terranes into eastern Panthalassa, and the early evolution of the North American Cordillera, *in* Cawood, P.A., and Kroner, A., eds., Earth Accretionary Systems in Space and Time: Geological Society, London, Special Publication 318, p. 273–307.

Colpron, M., Nelson, J.L., and Murphy, D.C., 2007, Northern Cordilleran terranes and their interactions through time: GSA Today, v. 17, p. 4–10, doi:10.1130/GSAT01704-5A.1.

Dickinson, W.R., 2000, Geodynamic interpretation of Paleozoic tectonic trends oriented oblique to the Mesozoic Klamath-Sierran continental margin in California, *in* Soreghan, M.J., and Gehrels, G.E., eds., Paleozoic and Triassic Paleogeography and Tectonics of Western Nevada and Northern California: Geological Society of America Special Paper 347, p. 209–245.

Dickinson, W.R., 2006, Geotectonic evolution of the Great Basin: Geosphere, v. 2, p. 353–368.

Dickinson, W.R., and Gehrels, G.E., 2009, U-Pb ages of detrital zircons in Jurassic eolian and associated sandstones of the Colorado Plateau: Evidence for transcontinental dispersal and intraregional recycling of sediment: Geological Society of America Bulletin, v. 121, p. 408–433, doi:10.1130/B26406.1.

Dickinson, W.R., and Lawton, T.F., 2001, Carboniferous to Cretaceous assembly and fragmentation of Mexico: Geological Society of America Bulletin, v. 113, p. 1142–1160, doi:10.1130/0016-7606(2001)113<1142:CTCAAF>2.0.CO;2.

Dickinson, W.R., Harbaugh, D.W., Saller, A.H., Heller, P.L., and Snyder, W.S., 1983, Detrital modes of upper Paleozoic sandstones derived from Antler orogen in Nevada: Implications for the nature of the Antler orogeny: American Journal of Science, v. 283, p. 481–509, doi:10.2475/ajs.283.6.481.

Dusel-Bacon, C., Hopkins, M.J., Mortensen, J.K., Dashevsky, S.S., Bressler, J.R., and Day, W.C., 2006, Paleozoic tectonic and metallogenic evolution of the pericratonic rocks of east-central Alaska and adjacent Yukon, *in* Colpron, M., and Nelson, J.L., eds., Paleozoic Evolution and Metallogeny of Pericratonic Terranes at the Ancient Pacific Margin of North America, Canadian and Alaskan Cordillera: Geological Association of Canada, Special Paper 45, p. 25–74.

Evans, J.G., and Theodore, T.G., 1978, Deformation of the Roberts Mountains Allochthon in North-Central Nevada: U.S. Geological Survey Professional Paper 1060, 18 p.

Fedo, C.M., Sircombe, K., and Rainbird, R., 2003, Detrital zircon analysis of the sedimentary record, *in* Hanchar, J.M., and Hoskin, P.W.O., eds., Zircon: Reviews in Mineralogy and Geochemistry, v. 53, p. 277–303.

Finney, S.C., 1998, The Laurentian affinity of the Roberts Mountains allochthon: Geological Society of America Abstracts with Programs, v. 30, no. 7, p. 150.

Finney, S.C., and Ethington, R.L., 1992, Graptolite and conodont faunas in Ordovician Vinini Formation, Roberts Mountains, central Nevada, demonstrate that the Roberts Mountains allochthon is not an exotic terrane: Fifth North American Paleontological Convention, abstracts and program, Field Museum of Natural History, v. 6, p. 97.

Finney, S.C., and Perry, B.D., 1991, Depositional setting and paleogeography of Ordovician Vinini Formation, central Nevada, *in* Cooper, J.D., and Stevens, C.H., eds., Paleozoic Paleography of the Western United States—II, Volume 2: Pacific Section, Society of Economic Paleontologists and Mineralogists book 67, p. 747–766.

Finney, S.C., Perry, B.D., Emsbo, P., and Madrid, R.J., 1993, Stratigraphy of the Roberts Mountains allochthon, Roberts Mountains and Shoshone Range, Nevada, *in* Lahren, M.M., Trexler, J.H., Jr., and Spinosa, C., eds., Crustal Evolution of the Great Basin and Sierra Nevada: Cordilleran/Rocky Mountain Section, Geological Society of America Guidebook, p. 197–230.

Gehrels, G.E., 2012, Detrital zircon U-Pb geochronology: Current methods and new opportunities, *in* Busby, C., and Azor, A., eds., Recent Advances in Tectonics of Sedimentary Basins: Hoboken, New Jersey, Blackwell Publishing, p. 47–62.

Gehrels, G.E., 2014, Detrital zircon U-Pb geochronology applied to tectonics: Annual Review of Earth and Planetary Sciences, v. 42, p. 127–149, doi:10.1146/annurev-earth-050212-124012.

Gehrels, G.E., and Pecha, M., 2014, Detrital zircon U-Pb geochronology and Hf isotope geochemistry of Paleozoic and Triassic passive margin strata of western North America: Geosphere, v. 10, p. 49–65, doi:10.1130/GES00889.1.

Gehrels, G.E., and Smith, M.T., 1987, “Antler” allochthon in the Kootenay arc?: Geology, v. 15, p. 769–770, doi:10.1130/0091-7613(1987)15<769:AAITKA>2.0.CO;2.

Gehrels, G.E., and Ross, G.M., 1998, Detrital zircon geochronology of Neoproterozoic to Permian miogeoclinal strata in British Columbia and Alberta: Canadian Journal of Earth Sciences, v. 35, p. 1380–1401, doi:10.1139/e98-071.

Gehrels, G.E., Dickinson, W.R., Riley, B.C.D., Finney, S.C., and Smith, M.T., 2000a, Detrital zircon geochronology of the Roberts Mountains allochthon, Nevada, *in* Gehrels, G.E., and Soreghan, M.J., eds., Paleozoic and Triassic Paleogeography and Tectonics of Western Nevada and Northern California: Boulder, Colorado, Geological Society of America, Special Paper 347, p. 19–42.

Gehrels, G.E., Dickinson, W.R., Darby, B.J., Harding, J.P., Manuszak, J.D., Riley, B.C.D., Spurlin, M.S., Finney, S.C., Girty, G.H., Harwood, D.S., Miller, M.M., Satterfield, J.I., Smith, M.T., Snyder, W.S., Wallin, E.T., and Wyld, S.J., 2000b, Tectonic implications of detrital zircon data from Paleozoic and Triassic strata in western Nevada and northern California, *in* Gehrels, G.E., and Soreghan, M.J., eds., Paleozoic and Triassic Paleogeography and Tectonics of Western Nevada and Northern California: Boulder, Colorado, Geological Society of America, Special Paper 347, p. 133–150.

Gehrels, G.E., Valencia, V.A., and Ruiz, J., 2008, Enhanced precision, accuracy, efficiency, and spatial resolution of U-Pb ages by laser ablation-multicollector-inductively coupled plasma-mass spectrometry: Geochemistry Geophysics Geosystems, v. 9, doi:10.1029/2007GC001805.

Gehrels, G.E., Blakey, R., Karlstrom, K.E., Timmons, J.M., Dickinson, B., and Pecha, M., 2011, Detrital zircon U-Pb geochronology of Paleozoic strata in the Grand Canyon, Arizona: Lithosphere, v. 3, p. 183–200, doi:10.1130/L121.1.

Gilluly, J., and Gates, O., 1965, Geology of the northern Shoshone Range, Nevada: U.S. Geological Survey Professional Paper 465, 153 p.

Goodge, J.W., and Vervoort, J.D., 2006, Origin of Mesoproterozoic A-type granites in Laurentia: Hf isotopic evidence: Earth and Planetary Science Letters, v. 243, p. 711–731, doi:10.1016/j.epsl.2006.01.040.

Guynn, J., and Gehrels, G.E., 2006, Comparison of detrital zircon age distribution using the K-S test: online manual published by the University of Arizona LaserChron Center: https://docs.google.com/file/d/0B9ezu34P5h8eZWZmOWUzOTItZDgyZi00NDRiLWI4ZTctNTljNTM5OTU1MGUz/edit?hl=enandpli=1.

Hoffman, P.F., 1989, Precambrian geology and tectonic history of North America, *in* Bally, A.W., and Palmer, A.R., eds., The Geology of North America—An Overview: Boulder, Colorado, Geological Society of America, The Geology of North America, v. A, p. 447–512.

Holm-Denoma, C.S., Hofstra, A.H., Noble, P.J., and Leslie, S.A., 2011, Paleozoic stratigraphy and kinematics of the Roberts Mountains allochthon in the Independence Mountains, northern Nevada, *in* Steininger, R., and Pennell, B., eds., Great Basin Evolution and Metallogeny: Geological Society of Nevada 2010 Symposium, p. 1039–1054.

Kay, M., 1951, North American geosynclines: Geological Society of America Memoir 48, 143 p.

Kent, D.M., 1994, Paleogeographic evolution of the cratonic platform—Cambrian to Triassic, *in* Mossop, G.D., and Shetsen, I., eds., Geological Atlas of the Western Canadian Sedimentary Basin, p. 69–86.

Ketner, K.B., 1966, Comparison of Ordovician eugeosynclinal and miogeosynclinal quartzites of the Cordilleran geosyncline: U.S. Geological Survey Professional Paper 550C, p. C54–C60.

Ketner, K.B., 1968, Origin of Ordovician quartzite in the Cordilleran miogeosyncline: U.S. Geological Survey Professional Paper 600B, p. B169–B177.

Lawton, T.F., Hunt, G.J., and Gehrels, G.E., 2010, Detrital zircon record of thrust belt unroofing in Lower Cretaceous synorogenic conglomerates, central Utah: Geology, v. 38, p. 463–466, doi:10.1130/G30684.1.

Linde, G.M., Cashman, P.H., Trexler, J.H., Jr., and Dickinson, W.R., 2014, Stratigraphic trends in detrital zircon geochronology of upper Neoproterozoic and Cambrian strata, Osgood Mountains, Nevada and elsewhere in the Cordilleran miogeocline: Evidence for early Cambrian uplift of the Transcontinental Arch: Geosphere, v. 10, p. 1402–1410, doi:10.1130/GES01048.1.

Ludwig, K.R., 2008, Isoplot 3.6, Berkeley Geochronology Center Special Publication 4, 77 p.

Lund, K., Aleinikoff, J.N., Evans, K.V., duBray, E.A., Dewitt, E.H., and Unruh, D.M., 2010, SHRIMP U-PB dating of recurrent Cryogenian and Late Cambrian–Early Ordovician alkalic magmatism in central Idaho: Implication for Rodinian rift tectonics: Geological Society of America Bulletin, v. 122, p. 430–453, doi:10.1130/B26565.1.

Madrid, R.J., 1987, Stratigraphy of the Roberts Mountains allochthon in north-central Nevada [Ph.D. dissertation]: Stanford, California, Stanford University, 336 p.

McKee, E.H., 1976, Geology of the northern part of the Toquima Range, Lander, Eureka, and Nye counties, Nevada: U.S. Geological Survey Professional Paper 931, 49 p.

Merriam, C.W., and Anderson, C.A., 1942, Reconnaissance survey of the Roberts Mountains, Nevada: Geological Society of America Bulletin, v. 53, p. 1675–1727, doi:10.1130/GSAB-53-1675.

Miller, E.L., and Larue, D.K., 1983, Ordovician quartzite in the Roberts Mountains allochthon, Nevada: Deep sea fan deposits derived from cratonal North America, *in* Stevens, C.H., ed., Pre-Jurassic rocks in Western North American Suspect Terranes: Society of Economic Paleontologists and Mineralogists, Pacific Section, 1983 convention, p. 91–102.

Mueller, P.A., Kamenov, G.D., Heatherington, A.L., and Richards, J., 2008, Crustal evolution in the southern Appalachian orogen: Evidence from Hf isotopes in detrital zircons: The Journal of Geology, v. 116, p. 414–422, doi:10.1086/589311.

Nelson, J.L., Colpron, M., Piercey, S.J., Dusel-Bacon, C., Murphy, D.C., and Roots, C.F., 2006, Paleozoic tectonic and metallogenetic evolution of pericratonic terranes in Yukon, northern British Columbia and eastern Alaska, *in* Colpron, M., and Nelson, J.L., eds., Paleozoic Evolution and Metallogeny of Pericratonic Terranes at the Ancient Pacific Margin of North America, Canadian and Alaskan Cordillera: Geological Association of Canada, Special Paper 45, p. 323–360.

Nilsen, T.H., and Stewart, J.H., 1980, The Antler orogeny—Mid-Paleozoic tectonism in western North America (Penrose Conference Report): Geology, v. 8, no. 6, p. 298–302, doi:10.1130/0091-7613(1980)8<298:TAOTIW>2.0.CO;2.

Noble, P.J., and Finney, S.C., 1999, Recognition of fine-scale imbricate thrusts in lower Paleozoic orogenic belts—An example from the Roberts Mountains allochthon, Nevada: Geology, v. 27, p. 543–546, doi:10.1130/0091-7613(1999)027<0543:ROFSIT>2.3.CO;2.

Oldow, J.S., 1984, Evolution of a late Mesozoic back-arc fold and thrust belt, northwestern Great Basin, U.S.A: Tectonophysics, v. 102, p. 245–274, doi:10.1016/0040-1951(84)90016-7.

Paradis, S., Bailey, S.L., Creaser, R.A., Piercey, S.J., and Schiarraza, P., 2006, Paleozoic magmatism and syngenetic massive sulphide deposits of the Eagle Bay assemblage, Kootenay terrane, southern British Columbia, *in* Colpron, M., and Nelson, J.L., eds., Paleozoic Evolution and Metallogeny of Pericratonic Terranes at the Ancient Pacific Margin of North America, Canadian and Alaskan Cordillera: Geological Association of Canada, Special Paper 45, p. 383–414.

Patchett, P.J., 1983, Importance of the Lu-Hf isotopic system in studies of planetary chronology and chemical evolution: Geochimica et Cosmochimica Acta, v. 47, p. 81–91, doi:10.1016/0016-7037(83)90092-3.

Patchett, P.J., and Tatsumoto, M., 1981, A routine high-precision method for Lu-Hf isotope geochemistry and chronology: Contributions to Mineralogy and Petrology, v. 75, p. 263–267, doi:10.1007/BF01166766.

Piercey, S.J., Nelson, J.L., Colpron, M., Dusel-Bacon, C., Roots, C.F., and Simard, R.L., 2006, Paleozoic magmatism and crustal recycling along the ancient Pacific margin of North America, northern Cordillera, *in* Colpron, M., and Nelson, J.L., eds., Paleozoic Evolution and Metallogeny of Pericratonic Terranes at the Ancient Pacific Margin of North America, Canadian and Alaskan Cordillera: Geological Association of Canada, Special Paper 45, p. 281–322.

Poole, F.G., 1974, Flysch deposits of Antler foreland basin, western United States, *in* Dickinson. W.R., ed., Tectonics and Sedimentation: Society of Economic Paleontologists and Mineralogists Special Publication 22, p. 58–82.

Poole, F.G., Stewart, J.H., Palmer, A.R., Sandberg, C.A., Madrid, R.A., Ross, R.J., Jr., Hintze, L.F., Miller, M.M., and Wrucke, C.T., 1992, Latest Precambrian to latest Devonian time: Development of a continental margin, *in* Burchfiel, B.C., Lipman, P.W., and Zoback, M.L., eds., The

Cordilleran Orogen: Conterminous U.S.: Boulder, Colorado, Geological Society of America, The Geology of North America, v. G-3, p. 9–56.

Rainbird, R.H., McNicoll, J., Theriault, R.J., Heaman, L.M., Abbott, J.G., Long, D.G.F., and Thorkelson, D.J., 1997, Pan-continental river system draining Grenville orogeny recorded by U-Pb and Sm-Nd geochronology of Neoproterozoic quartz arenites and mudrocks, northwestern Canada: The Journal of Geology, v. 105, p. 1–17, doi:10.1086/606144.

Rainbird, R.H., Cawood, P., and Gehrels, G., 2012, The great Grenvillian sedimentation episode: Record of supercontinent Rodinia's assembly, *in* Busby, C., and Azor, A., eds., Tectonics of Sedimentary Basins: Recent Advances: Blackwell Publishing Ltd., p. 583–601.

Roberts, R.J., Hotz, P.E., Gilluly, J., and Ferguson, H.G., 1958, Paleozoic rocks of north-central Nevada: The American Association of Petroleum Geologists Bulletin, v. 42, p. 2813–2857.

Rohr, T.S., Andersen, T., and Dypvik, H., 2008, Provenance of Lower Cretaceous sediments in the Wandel Sea Basin, North Greenland: Journal of the Geological Society, London, v. 165, p. 755–767, doi:10.1144/0016-76492007-102.

Rohr, T.S., Andersen, T., Dypvik, H., and Embry, A.F., 2010, Detrital zircon characteristics of the Lower Cretaceous Isachsen Formation, Sverdrup Basin: Source constraints from age and Hf isotope data: Canadian Journal of Earth Sciences, v. 47, p. 255–271, doi:10.1139/E10-006.

Ross, G.M., 1991, Precambrian basement in the Canadian Cordillera: An introduction: Canadian Journal of Earth Sciences, v. 28, p. 1133–1139, doi:10.1139/e91-103.

Scherer, E., Munker, C., and Mezger, K., 2001, Calibrating the Lu-Hf clock: Science, v. 293, p. 683–687, doi:10.1126/science.1061372.

Schuchert, C., 1923, Sites and nature of the North American geosynclines: Geological Society of America Bulletin, v. 34, p. 151–229, doi:10.1130/GSAB-34-151.

Sloss, L.L., ed., 1988, Tectonic evolution of the craton in Phanerozoic time, *in* Sloss, L.L., ed., Sedimentary Cover—North American Craton: U.S.: Boulder, Colorado, Geological Society of America, The Geology of North America, v. D-2.

Söderlund, U., Patchett, P.J., Vervoort, J.D., and Isachsen, C.E., 2004, The ^{176}Lu decay constant determined by Lu-Hf and U-Pb isotope systematics of Precambrian mafic intrusions: Earth and Planetary Science Letters, v. 219, p. 311–324, doi:10.1016/S0012-821X(04)00012-3.

Speed, R.C., and Sleep, N.H., 1982, Antler orogeny and foreland basin: A model: Geological Society of America Bulletin, v. 93, p. 815–828, doi:10.1130/0016-7606(1982)93<815:AOAFBA>2.0.CO;2.

Todt, M.K., and Link, P.K., 2013, Sedimentary provenance of the Upper Cambrian Worm Creek Quartzite, Idaho, using U-Pb and Lu-Hf isotopic analysis of zircon grains: Northwest Geology, v. 42, p. 293–298.

Trexler, J.H., Jr., Cashman, P.H., Cole, J.C., Snyder, W.S., Tosdal, R.M., and Davydov, V.I., 2003, Widespread effects of middle Mississippian deformation in the Great Basin of western North America: Geological Society of America Bulletin, v. 115, p. 1278–1288, doi:10.1130/B25176.1.

Van Schmus, W.R., Bickford, M.E., Sims, P.K., Anderson, J.L., Shearer, C.K., and Treves, S.B., 1993, Proterozoic geology of the western midcontinent region, *in* Reed, J.C., Bickford, M.E., Houston, R.S., Link, P.K., Rankin, D.W., Sims, P.K., and Van Schmus, W.R., eds., Precambrian Conterminous U.S.: Boulder, Colorado, Geological Society of America, The Geology of North America, v. C-2, p. 239–259.

Vervoort, J.D., and Blichert-Toft, J., 1999, Evolution of the depleted mantle: Hf isotope evidence from juvenile rocks through time: Geochimica et Cosmochimica Acta, v. 63, p. 533–556, doi:10.1016/S0016-7037(98)00274-9.

Vervoort, J.D., and Patchett, P.J., 1996, Behavior of hafnium and neodymium isotopes in the crust: Constraints from crustally derived granites: Geochimica et Cosmochimica Acta, v. 60, p. 3717–3733, doi:10.1016/0016-7037(96)00201-3.

Vervoort, J.D., Patchett, P.J., Blichert-Toft, J., and Albarede, F., 1999, Relationships between Lu-Hf and Sm-Nd isotopic systems in the global sedimentary system: Earth and Planetary Science Letters, v. 168, p. 79–99, doi:10.1016/S0012-821X(99)00047-3.

Vervoort, J.D., Patchett, P.J., Soderlund, U., and Baker, M., 2004, Isotopic composition of Yb and the determination of Lu concentrations and Lu/Hf ratios by isotope dilution using MC-ICPMS: Geochemistry Geophysics Geosystems, v. 5, Q11002, doi:10.1029/2004GC000721.

Villeneuve, M.E., Ross, G.M., Theriault, R.J., Miles, W., Parrish, R.R., and Broome, J., 1993, Tectonic subdivision and U-Pb geochronology of the crystalline basement of the Alberta basin, western Canada: Geological Survey of Canada, Bulletin 447, 86 p.

Whitmeyer, S.J., and Karlstrom, K.E., 2007, Tectonic model for the Proterozoic growth of North America: Geosphere, v. 3, p. 220–259.

Woodhead, J.D., and Hergt, J.M., 2005, A preliminary appraisal of seven natural zircon reference materials for in situ Hf isotope determination: Geostandards and Geoanalytical Research, v. 29, no. 2, p. 183–195, doi:10.1111/j.1751-908X.2005.tb00891.x.

Woodhead, J., Hergt, J., Shelley, M., Eggins, S., and Kemp, R., 2004, Zircon Hf-isotope analysis with an excimer laser, depth profiling, ablation of complex geometries, and concomitant age estimation: Chemical Geology, v. 209, p. 121–135, doi:10.1016/j.chemgeo.2004.04.026.

Wright, J., and Wyld, S., 2006, Gondwana, Iapetan, Cordilleran interactions: A geodynamic model for the Paleozoic tectonic evolution of the North American Cordillera, *in* Haggart, J., Enkin, R., and Monger, J., eds., Paleogeography of the North American Cordillera: Evidence for and against Large-Scale Displacements: Geological Association of Canada Special Paper 46, p. 377–408.

Yonkee, W.A., Dehler, C.D., Link, P.K., Balgord, E.A., Keeley, J.A., Hayes, D.S., Wells, M.L., Fanning, C.M., and Johnston, S.M., 2014, Tectono-stratigraphic framework of Neoproterozoic to Cambrian strata, west-central U.S.: Protracted rifting, glaciation, and evolution of the North American Cordilleran margin: Earth-Science Reviews, v. 136, p. 59–95, doi:10.1016/j.earscirev.2014.05.004.